Computational Mathematics for Learning and Data Analysis

Implementation of a Neural Network optimized through Stochastic Gradient Descent and Conjugate Gradient Descent

Sabrina Briganti - 465214 - brisabry5@gmail.com
Gianmarco Ricciarelli - 555396 - gianmarcoricciarelli@gmail.com

May 20, 2019

Contents

Chapter 1

The Artificial Neural Network

In this first Chapter, we provide some informations about the Artificial Neural Network, i.e. a fully connected Multilayer Perceptron, we implemented from scratch. We'll describe both the network's structure and the algorithm we used in order to make our network *learn* from the data used during the testing and validation phases. Finally we'll present the loss function we have chosen for our network, and we'll provide and explanation on how it is differentiable. We'll use the notation proposed in [9].

1.1 The ANN's structure

Since we have to write from scratch an *Artificial Neural Network*, ANN for short, we have considered some alternatives before choosing the network's final structure. We agreed on a structure composed by:

- one *input layer*;
- two *hidden layers*;
- one *output layer*;

As convention, the number of units in the input layer is egual to the number of features of the dataset that is used for the learning, validation and testing phases. The two hidden layers contain, respectively, four and eight *hidden neurons*, following the convention of putting an increasing series of powers of two as number of hidden units per layer. The number of neurons for the output layer depends on the kind of task the network is trying to fullfil. In the case of a *classification task*, like the MONKS dataset [5], we have decided to put one unit in the output layer, while in the case of a *regression task*, like the CUP dataset, we have decided to put two units in the output layer. As we have seen studying the papers and books for gathering the necessary knowledge for the project, as [9, 11, 14], choosing to consider the network's structure as an *hyperparameter*, that is, a variable, could lead to a series of difficult choices during the validation phase, so we have decided to fix the ANN structure to the one described for both the task we have to fullfil, changing only the number of units in the output layer from task to task. In figure 1.1 you can see our ANN's graph for the classification task.

1.2 Initializing the Network

As we know from [9, 11, 14], an ANN is composed by a set of weights $\mathbf{W}_i$, and a set of biases $\mathbf{b}_i$, $i \in \{1, \dots, l\}$, with l representing the ANN's number of layers. Although it is common practice to initialized the network's weights and biases to random, small, values,

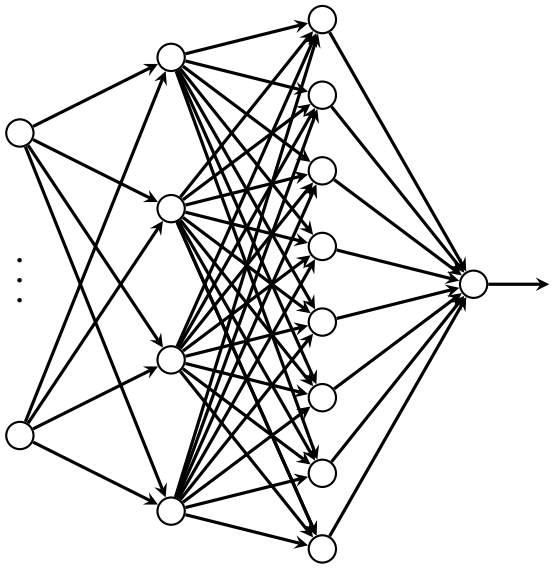

Figure 1.1: The ANN's structure for the classification task, the majority of the input nodes are omitted because they vary from dataset to dataset.

we have decided to follow the *normalized initialization*, as described in [8, 9], which defines the initial values for the weights and the biases for each layer in the uniform distribution taken in the range

$$W \sim U\left[-\frac{\sqrt{6}}{\sqrt{m+n}},\ \frac{\sqrt{6}}{\sqrt{m+n}}\right]$$

with m and n, representing the number of inputs and outputs for each layer. This heuristic is designed to compromise between the goal of initializing all layers to have the same activation variance and the goal of initializing all layers to have the same gradient variance. The formula is derived using the assumption that the network consists only of a chain of matrix multiplications, with no nonlinearities. Other than this kind of initialization, we also make available the standard *random initialization* for creating a network, described at the beginning of this §, which initialize the weights and the biases for each layer in the uniform distribution taken in the range

$$W \sim U\left[-0.7,\ 0.7\right].$$

1.3 The back-propagation algorithm

The learning procedure for our ANN essentialy consist in two distinct phases:

1. compute the network's *gradient*, that is, the derivative of the cost function $\nabla_\theta J(\theta)$, with θ representing the ANN's hyperparameters, with respect to every network's unit using the well known *back-propagation algorithm*, described by algorithm 1 and 2;

2. optimize the information gathered during the first phase using a distinct optimizer, chosen among the *Stochastic Gradient Descent* and the *Conjugate Gradient Method*, as described in Chapter 2;

For computing the gradient we have chosen to use the well known *backpropagation algorithm*, firstly introduced in [20] and described in [9, 11, 14]. This algorithm is also composed by two phases, a first phase, that is, the *forward propagation*, in which the feature vector

$\mathbf{x}$ given in input has to flow from the input layer through the hidden layers and, finally, the output layer, giving the approximation $\hat{\mathbf{y}}$ as output, and a second one, that is, the *back-propagation*, which allows the information to flow backward through the network in order to compute the gradient by applying the Chain Rule of Calculus, that is, a technique for computing the derivative of a composition of functions.

Algorithm 1 Forward propagation through a typical (deep) neural network and the computation of the cost function. Here $L(\hat{\mathbf{y}}, \mathbf{y})$ represents the loss function evaluated using both $\mathbf{y}$ and $\hat{\mathbf{y}}$ as inputs, more details about that will be provided in §1.5. The function f applied on line 5 represents the layer's *activation function*, while $\lambda\Omega(\theta)$ represents the network's regularization term, with θ representing the ANN's hyperparameters.

1: **procedure** FORWARD PROPAGATION(l, $\mathbf{W}_i$ $i \in \{1, \dots, l\}$, $\mathbf{b}_i$ $i \in \{1, \dots, l\}$, $\mathbf{x}$, $\mathbf{y}$)
2: $\quad \mathbf{h}_0 = \mathbf{x}$
3: $\quad$ **for** $k = 1, \dots, l$ **do**
4: $\quad\quad \mathbf{a}_k = \mathbf{b}_k + \mathbf{W}_k \mathbf{h}_{k-1}$
5: $\quad\quad \mathbf{h}_k = f(\mathbf{a}_k)$
6: $\quad \hat{\mathbf{y}} = \mathbf{h}_l$
7: $\quad J = L(\hat{\mathbf{y}}, \mathbf{y}) + \lambda\Omega(\theta)$

Since each one of the ANN's layers has its own *activation function*, that is, a function that has to be applyied to the output of every layer's neuron, it is particularly usefull to think of the ANN like a composition of functions, and, for this reason, the Chain Rule of Calculus play a decisive role in the gradient's computation by back-propagation. It is import to note that with the term back-propagation we mean only the method for computing the gradient, not the whole learning algorithm. We now provide the pseudocode for the forward propagation and the back-propagation phases, as shown in algorithms 1 and 2.

Algorithm 2 Backward computation for the (deep) neural network of algorithm 1. Here, the $\odot$ symbol represents the element-wise (Hadamard) product, while $\nabla_{\hat{\mathbf{y}}} J = \nabla_{\hat{\mathbf{y}}} L(\hat{\mathbf{y}}, \mathbf{y})$ represents the gradient of the loss function computed with respect to the output $\hat{\mathbf{y}}$. $\nabla_{\mathbf{b}_k} J$, $\nabla_{\mathbf{W}_k} J$ and $\nabla_{\mathbf{h}_{k-1}} J$ represents the gradient of the loss function computed with respect to, respectively, $\mathbf{b}_k$, $\mathbf{W}_k$ and $\mathbf{h}_{k-1}$, and finally $\nabla_{\mathbf{b}_k} \Omega(\theta)$ and $\nabla_{\mathbf{W}_k} \Omega(\theta)$ represents the gradient of the ANN's hyperparameters computed with respect to, respectively, $\mathbf{b}_k$ and $\mathbf{W}_k$.

1: **procedure** BACKWARD PROPAGATION
2: $\quad \mathbf{g} \leftarrow \nabla_{\hat{\mathbf{y}}} J = \nabla_{\hat{\mathbf{y}}} L(\hat{\mathbf{y}}, \mathbf{y})$
3: $\quad$ **for** $k = l, l-1, \dots, 1$ **do**
4: $\quad\quad \mathbf{g} \leftarrow \nabla_{\mathbf{a}_k} J = \mathbf{g} \odot f'(\mathbf{a}_k)$
5: $\quad\quad \nabla_{\mathbf{b}_k} J = \mathbf{g} + \lambda \nabla_{\mathbf{b}_k} \Omega(\theta)$
6: $\quad\quad \nabla_{\mathbf{W}_k} J = \mathbf{g}\mathbf{h}_{k-1}^T + \lambda \nabla_{\mathbf{W}_k} \Omega(\theta)$
7: $\quad\quad \mathbf{g} = \nabla_{\mathbf{h}_{k-1}} J = \mathbf{W}_k^T \mathbf{g}$

1.4 The activation functions

As we have mentioned in §1.3, each one of the ANN's layers has an *activation function*, that is, a function that is applied to $\mathbf{a}_k$ in order to obtain $\mathbf{h}_k$, with $k \in \{1, \dots, l\}$. We can say that an activation function of a node defines the output of that node, and maps $\mathbf{a}_k$ into the desired range. For being chosen as an activation function, a function has to possess a series of properties, such as

- *nonlinearity*: when the activation function is non-linear, then a two-layer neural

network can be proven to be a universal function approximator;

- *range*: when the range of the activation function is finite, gradient-based training methods, such as the ones described in chapter 2, tend to be more stable, because pattern presentations significantly affect only limited weights;
- *continuously differentiable*: since the functions have to be envolved in the Chain Rule of Calculus during the gradient's computation in the back-propagation algorithm;

There are many functions that can be used as activation functions for an ANN; we have chosen to utilize the well known *logistic function*, i.e. the *sigmoid function*, which is computed as

$$f(x) = \sigma(x) = \frac{1}{1 + e^{-x}}$$
$$f'(x) = \sigma'(x) = f(x)(1 - f(x)),$$

and is defined in the range (0, 1). As introduced in §1.3, we can think the ANN as a *composition* of activation functions, and, since we have stated that each one of the network's layers uses the logistic function as activation function, we can represent the ANN as

$$\sigma_l \circ \sigma_{l-1} \circ \cdots \circ \sigma_1$$

with l representing the total number of layers in the network and σ representing the logistic function.

1.5 The Loss function

It §1.3 we have referred to the *Loss function* as to a function that takes as input the ANN's output vector $\hat{\mathbf{y}}$ and the *ground truth* vector $\mathbf{y}$, that is, the vector containing the desired output for the network. But what essentially is a Loss function? As a matter of fact, the Loss function can be considered like one way of measuring the performance, or equivalently the error, of the model that utilizes it, an ANN in this case. There are various types of Loss functions, for our network we have decided to use a well known function: the *Mean Squared Error*, MSE for short, for both the classification and the regression tasks. The MSE is obtained with the formula

$$\text{MSE} = \frac{1}{m} \sum_{i=1}^{m} (\hat{\mathbf{y}} - \mathbf{y})_i^2 ,$$

where m represents the number of samples for which we computed the output $\hat{\mathbf{y}}$. We can represent this functions also as a composition of the square function and the Euclidean norm by writing the latter formula as

$$\text{MSE} = \frac{1}{m} ||\hat{\mathbf{y}} - \mathbf{y}||_2^2.$$

Since this formula is used for computing the performances of our models, our primary goal is to minimize its output as much as possible by computing the gradient during the backward propagation step of the back-propagation algorithm, as described in §1.3. Of course, in order to do so, it must be a *differentiable* function. The gradient for the MSE with respect to $\hat{\mathbf{y}}$ is defined as:

$$\nabla_{\hat{\mathbf{y}}} \text{MSE}\,(\hat{\mathbf{y}},\ \mathbf{y}) = \hat{\mathbf{y}} - \mathbf{y}.$$

1.5.1 Properties of the Loss function

Here we discuss the relevant properties of the Loss function we have chosen for our model.

- **Continuity**. As we introduced in this section, our Loss function is a function in two variables, $\hat{\mathbf{y}}$ and $\mathbf{y}$, respectively. A function f in two variables is L-Lipschitz continuous if there exists a constant L such that

  $$||f(\mathbf{x}_1, \mathbf{y}_1) - f(\mathbf{x}_2, \mathbf{y}_2)|| \leq L(||\mathbf{x}_1 - \mathbf{x}_2|| + ||\mathbf{y}_1 - \mathbf{y}_2||) \quad \forall (\mathbf{x}_1, \mathbf{y_1}), (\mathbf{x}_2, \mathbf{y_2}) \in \textbf{dom } f.$$

  Being the MSE a composition of the square function and the Euclidean norm, because of the squaring, the function is Lipschitz continuous only if we restrict its domain to a bounded set. Since, as described in §1.4, each network's layer uses the sigmoid function, which is a squashing function that bounds every layer's output in the range $(0,\ 1)$, the MSE can be considered as a continous function.

- **Differentiability**. Again, being the sigmoid function the one used by the ANN, and since the sigmoid function is continuously differentiable with bounded Lipschitz continuous derivative, we can consider the MSE as a differentiable function, being the network a composition of continuously differentiable functions.

- **Convexity**. We recall that, for $h : \mathbb{R}^k \to \mathbb{R}$, $g_i : \mathbb{R}^n \to \mathbb{R}$, the function:

  $$f(\mathbf{x}) = h(g_1(\mathbf{x}), \ldots, g_k(\mathbf{x}))$$

  is convex if **dom** $h = \mathbb{R}^k$, **dom** $g = \mathbb{R}^n$, h is convex, h is non-decreasing in each argument and g_i are convex. For the aforesaid result, the squared Euclidean distance is convex, as any distance is non-negative and the square function is convex and increasing for non-negative values; however, when composed with another function it may not be convex. The functions that compose the network, that is, the sigmoid functions, are not convex functions, hence we can conclude that, for our network, the MSE is a not convex function.

Chapter 2

Optimizers

2.1 Stochastic Gradient Descent

When choosing an optimizer, the *Stochastic Gradient Descent*, SGD for short, is a quite common choice. It is not the best though, since, as proved by the last developments in the machine learning field, its convergence's rate is quite slow. Said that, it is also true that it allows to finds a very low value of the cost function quickly enough.
The algorithm 3 shows the standard SGD version implemented, as described in [9], supporting both *momentum* and *regularization*. [13]
SGD is an extension of the *Gradient Descent Algorithm* (GD). It is an iterative first-order optimization technique, usefull to minimize the objective Loss function.
The main goal is, indeed, to minimize the Loss function, in order to obtain a neural network with good generalization property:

$$\min_{\mathbf{W} \in \mathbb{R}^n} \quad L(\mathbf{W}), \tag{2.1}$$

where L is the Loss function and $\mathbf{W}$ are the synaptic weights of the network.
The way to achieve this result, is to identify and compute a local minimum, moving along the direction of the steepest descent of the function, that is the negative gradient $-\nabla L(\mathbf{W})$.
Of course, in order to find a local minimum, it is necessary to update the synaptic weights $\mathbf{W}$ at each iteration as $\mathbf{W} = \mathbf{W} + \Delta\mathbf{W}$.
The correction applied to the each one of the weights is defined as follows, taking a step in the opposite direction of the cost gradient:

$$\Delta w_{ji} = -\eta \frac{\partial L}{\partial w_{ji}}, \tag{2.2}$$

where η is the learning rate. The latter one is a fundamental hyperparameter which has to been chosen wisely, since it represents how much is right to move along the descent direction: too much and the procedure will be vain, missing the minimum; too little and the converge will be slow.
Unlike the GD algorithm, that could get a longer time to converges to the minimum because of the potentially big number of training examples, the SGD algorithm requires only the evaluation of one example for epochs (on-line mode).
Here, however, we refer to SGD even when using the entire or just a subset of training dataset (batch or mini batch).
The name stochastic derives from the fact that the samples are randomly selected, bringing to an approximation of the true gradient, estimated using a small set of samples. This is also the reason of the typical zig-zag pattern in the path towards the minimum of the Loss function, as visible in Fig.2.1.

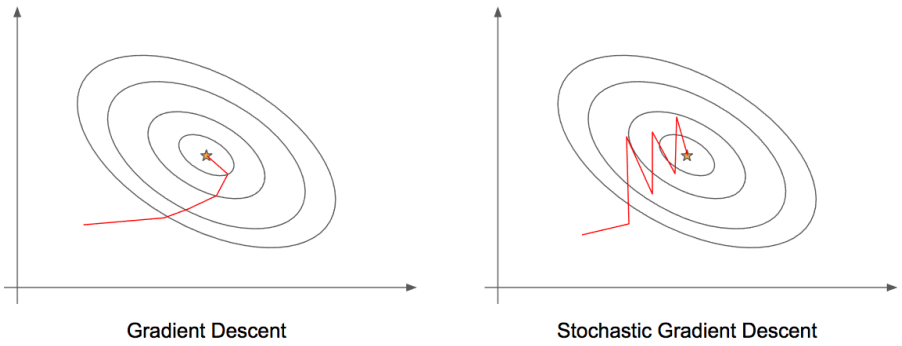

Figure 2.1: The different trajectories from GD and SGD.

For what concernes the convergence of the stochastic gradient descent algorithm, it depends on the choice of η: it is necessary to gradually decrease the learning rate over the epochs for ensure convergence. A sufficient condition to guarantee convergence of SGD is that the sequence of decreasing learning rates satisfy:

$$\sum_{t=1}^{\infty} \eta_t = \infty \quad \text{and} \quad \sum_{t=1}^{\infty} \eta_t^2 < \infty \tag{2.3}$$

Futhermore, if we assume that the Hessian matrix of the Loss function is strictly positive definite at the optimum, which means that the Loss function is strogly convex, the convergence rate is $O(\frac{1}{k})$, with k as the number of epochs in the training. Otherwise, relaxing this assumption in presence of a convex problem, the convergence rate becomes $O(\frac{1}{\sqrt{k}})$[9, 15, 21].
Unfortunatly, as we showed in §1.5.1, our objective function is not convex, so we can't rely on what has been written before. Anyway, this issue seems to be overcomed: as proved in [2], the SGD is convergent even in presence of nonconvex functions. If the algorithm is run with a stepsize sequence satisfying Eq.2.3 and the following assumptions hold:

Assumption 1 - *If the level set* $\mathcal{L} = \{w : L(\boldsymbol{W}) \leq L(\boldsymbol{W}_1)\}$ *is bounded, in some neighborhood* $\mathcal{N}$ *of* $\mathcal{L}$ *the objective function* L *is continuously differentiable, and its gradient is Lipschitz continuous, there exist a constant* $B > 0$ *s.t.* $\|\nabla L(\boldsymbol{W}) - \nabla L(\widetilde{\boldsymbol{W}})\| \leq B\|\boldsymbol{W} - \widetilde{\boldsymbol{W}}\|, \forall \boldsymbol{W}, \widetilde{\boldsymbol{W}} \in \mathcal{N}$;

Assumption 2 - *The Loss function* L *and SGD satisfy:*

- *The sequence of weights* $\boldsymbol{W}_k$ *is contained in an open set over which* L *is bounded below by a scalar value* L_{inf}*, that means the function is bounded below over the region explored by the algorithm;*
- *There exist scalars* $\mu_G \geq \mu > 0$ *s.t.,* $\forall k \in \mathbb{N}$,

$$\nabla L(\boldsymbol{W}_k)^T \mathbb{E}_{\xi_k}[\boldsymbol{g}(\boldsymbol{W}_k, \xi_k)] \geq \mu \|\nabla L(\boldsymbol{W}_k)\|^2 \text{ and} \tag{2.4}$$

$$\|\mathbb{E}_{\xi_k}[\boldsymbol{g}(\boldsymbol{W}_k, \xi_k)]\| \leq \mu_G \|\nabla L(\boldsymbol{W}_k)\|, \tag{2.5}$$

- *There exist scalars* $M \geq 0$ *and* $M_G \geq 0$ *s.t.:*

$$\|\mathbb{V}_{\xi_k}[\boldsymbol{g}(\boldsymbol{W}_k, \xi_k)]\| \leq M + M_G \nabla L(\boldsymbol{W}_k)\|^2, \forall k \in \mathbb{N}, \tag{2.6}$$

then the following property is garanteed:

$$\lim_{k\to\infty} \mathbb{E}[\|\nabla L(\mathbf{W}_k)\|^2] = 0$$

that is the convergence of the algorithm.
As we introduced in section 1.4, each one of the units of our ANN uses the sigmoid function as activation function. This function bounds every layer's output in the range $(0, 1)$. In section 1.5, we have proved that our loss function is both Lipschitz continuous and differentiable. We can conclude that assumption 1 is respected. The first requirement of assumption 2 is respected, being L bounded in the interval $(0, 1)$, that is, having L_{inf} eguals to 0. The second requirement means that the vector $-\mathbf{g}$ (the extimate of the real gradient vector) is a direction of sufficient descent for L with a norm comparable to the norm of the gradient, while the third requirement restricts the variance of $\mathbf{g}$.
A property of SGD is that the computation time per update does not grow with the number of training examples, allowing convergence even in presence of a large dataset.

Algorithm 3 Stochastic Gradient Descent Algorithm. The learning rate η, the α term and the maximum number of epochs are given.

procedure STOCHASTIC GRADIENT DESCENT
  Initialize $\mathbf{W}$ and $\mathbf{v}$
  $k \leftarrow 0$
  while $k < max\_epochs$ **do**
    Sample a minibatch of m training examples $\{(x_0, y_0), (x_1, y_1), ..., (x_m, y_m)\}$
    if Nesterov Momentum **then**
      $\mathbf{W} \leftarrow \mathbf{W} + \alpha\mathbf{v}$
    Compute gradient estimate: $\mathbf{g} \leftarrow \frac{1}{m}\nabla \sum_i L(\mathbf{W})$
    Compute velocity update: $\mathbf{v} \leftarrow \alpha\mathbf{v} - \eta\mathbf{g}$
    Apply update: $\mathbf{W} \leftarrow \mathbf{W} + \mathbf{v}$

2.1.1 Momentum

When computing the adjustment of the synaptic weights $\Delta\mathbf{W}$ as in Eq. 2.3, the choice of the learning rate η influences the convergence of the SGD algorithm. The smaller is η, the smaller will be the changes in the matrix of weights and the rate of learning, but the smoother will be the trajectory.
On the contrary, a bigger η will bring to a faster convergence, but also to an oscillatory behaviour.
A way to accelerate the SGD is the use of the *Classical Momentum* (CM), a first order optimization technique which accelerate gradient descent, and so the learning rate of the final training.
It consists in the adjustment of the new weigths through a velocity vector $\mathbf{v}$ that accumulates the gradient elements in the directions of reduction of the Loss function, and in a momentum coefficient $\alpha \in [0, 1]$: the larger is α, the more the previous gradients affect the current direction.
In this case, the classical momentum is given by:

$$\mathbf{v}_k = \alpha\mathbf{v}_{k-1} + \eta\nabla L(\mathbf{W}_k). \tag{2.7}$$

The new synaptic weights are then updated as:

$$\mathbf{W}_k = \mathbf{W}_{k-1} + \mathbf{v}_k. \tag{2.8}$$

A variant of the CM algorithm, is the *Nesterov's Accelerated Gradient* (NAG), which allows to avoid the oscillatory behaviour in the trajectory computed with CM, as visible in Fig.2.2b
The velocity vector $\mathbf{v}$ is computed as:

$$\mathbf{v}_k = \alpha \mathbf{v}_{k-1} + \eta \nabla L(\mathbf{W}_k + \alpha \mathbf{v}_{k-1}). \tag{2.9}$$

The update of the weights $\mathbf{W}$ follows the one described in Eq. 2.8.
The variant respect Eq. 2.7, shown in Fig.2.2a, is given by the fact that the gradient ∇L is evaluated after the current velocity is applied: NAG first update the $\mathbf{W}_k$, making a jump in the direction of the previous accumulated gradient, and then evaluate the gradient in that point and makes a correction. This procedure allows it to change velocity vector $\mathbf{v}_k$ in a faster way.
We now discuss the convergence of a SGD using both classic momentum or Nesterov's accelerated gradient by providing some of the results illustrated in [24], in particular the ones describing the case of the optimization of a non-convex function, that is, our case. We denote by $\mathbb{E}[\cdot]$ the expected value taken with respect to the distribution of the random variable whose observed value represents the choice of a particular minibatch at step k and by $\mathbf{g}^{(k)}$ the estimate of the true full-batch gradient $\nabla F(\theta^{(k)})$.

Theorem 2.1.1 (Convergence of Gradient Methods for Non-Convex Functions) *Suppose L is a function with B-Lipschitz continuous gradient, $\mathbb{E}\left[||\mathbf{g}_i - \nabla L(\boldsymbol{w}_i)||^2\right] \leq \delta^2$, and $||\nabla L(\boldsymbol{w}_i)|| \leq G$ for any $\boldsymbol{w}_i \in \boldsymbol{W}$. Then, for any constant $C > 0$, running for k iteration the stochastic gradient method*

1. *with step size $\eta = min\left\{1/(2B),\ C/\sqrt{k+1}\right\}$ yields*

$$min_{i=0,\dots,k}\mathbb{E}\left[||\nabla L(\boldsymbol{w}_i)||^2\right] \leq \frac{2(L(\boldsymbol{w}_0)) - L_*}{k+1} max\left\{2B,\ \frac{\sqrt{k+1}}{C}\right\} + \frac{CB\delta^2}{\sqrt{k+1}} \text{ and}$$

2. *with step size $\eta = min\left\{(1-\alpha)/(2B),\ C/\sqrt{k+1}\right\}$ and a momentum $\alpha \in [0,1)$ yelds*

$$min_{i=0,\dots,k}\mathbb{E}\left[||\nabla F(\boldsymbol{w}_i)||^2\right] \leq \frac{2(L(\boldsymbol{w}_0) - L_*)(1-\alpha)}{k+1} max\left\{\frac{2B}{1-\alpha},\ \frac{\sqrt{k+1}}{C}\right\} + \frac{C}{\sqrt{k+1}} \frac{B\alpha^2 + B\delta^2(1-\alpha)^2}{(1-\alpha)^3}$$

Theorem 2.1.1 ensures that SGD with or without momentum converges in expectation for non-convex functions.
It's worth to underline that, in case of batch mode and convex functions, Nesterov momentum brings the rate of convergence from $O(\frac{1}{k})$ (after k steps) to $O(\frac{1}{k^2})$[17].

2.1.2 Regularization

In order to garantee a tradeoff between goodness and complexity of the model, the regularization is allowed in the network. This choice is important to ensure that the model doesn't grow too much in complexity.
Regularization, in fact, adds a penalty as the model's complexity increases, forcing some weights to take values close to zero, if they have little influence on the newtork performance and so resulting in poor generalization.
It basically modifies the objective Loss functions as follows:

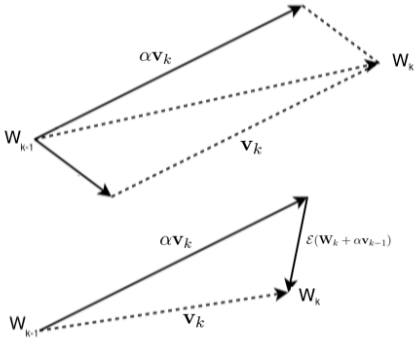

(a) The classical momentum on top and the Nesterov Accelerated gradient on bottom.

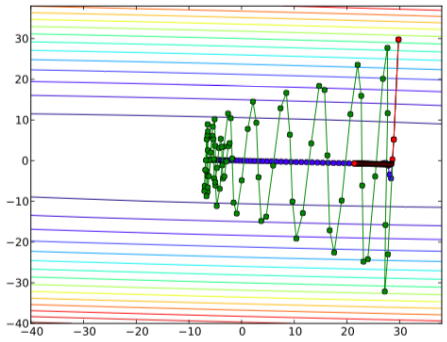

(b) The trajectory from CM (in green) and the one from NAG (in blue).

$$\min_{\mathbf{W} \in \mathbb{R}^n} \quad L(\mathbf{W}) + \lambda \Omega(\mathbf{W}) \tag{2.10}$$

where $\Omega(\mathbf{W})$ is a complexity penalty term based of the weights, and λ is a parameter which tells how much importance must have the complexity penalty term.
Two kinds of regularization are tipically used:

- *L1*: also called Lasso Regression, which results in $\Omega(\mathbf{W}) = \sum_{i=1}^{k} |w_i| = \|\mathbf{W}\|_1$;
- *L2*: also known as Ridge Regression, which results in $\Omega(\mathbf{W}) = \sum_{i=1}^{k} w_i^2 = \|\mathbf{W}\|_2^2$.

The addition of squared terms to the Loss function of Eq.1.5 in the Ridge Regression, returns again a smooth continous and differentiable function.
However, the Lasso penalty, which pushes several elements of $\mathbf{W}$ to be exactly zero, making the result a sparse parameter vector, is not differentiable. So, since when applied to the Loss function, it returns a non-smooth function, it hasn't been tested on SGD[22].

2.2 Nonlinear Conjugate Gradient

An intresting optimization ables to lead to an improvement of the performances of the neural network, is the use of high-order information during the training phase: this brings to a more accurate choice of the search direction and of the step size, by using information from the second order approximation.
In order to avoid the expensive computation of the inverse of the Hessian, we can use the *Conjugate Gradient* methods, which are a class of iterative second-order optimization methods, derived from the steepest-descent algorithm, that ensure low memory requirements.
In this way, the adjustment to the synaptic weights of the network is computed as:

$$\Delta \mathbf{W} = \alpha \mathbf{d}, \tag{2.11}$$

where α is the learning rate and $\mathbf{d}$ is the new direction found.
In our case, the nonlinear conjugate gradient methods are designed to solve the minimization problem defined in Eq.2.1.
As showed in the pseudocode 4, the iterative formula generates a sequence of weights $\{W_k\}$, for every epoch of training k, as:

$$\mathbf{W}_{k+1} = \mathbf{W}_k + \alpha_k \mathbf{d}_k, \quad k = 0, 1, ..., \tag{2.12}$$

where α_k is a learning rate and $\mathbf{d}_k$ is a descent direction. These are the new synaptic weights computed with the adjustment of Eq.2.11.

Algorithm 4 Nonlinear Conjugate Gradient Algorithm. The maximum number of epochs and the tolerance are given.

procedure NONLINEAR CONJUGATE GRADIENT
  Initialize $\mathbf{W}_0$ and L_g
  $k \leftarrow 0$, $g_0 \leftarrow 0$
  while $k < max\_epochs$ **do**
    Evaluate the Loss function L_k and its gradient $\mathbf{g}_k$
    if $L_k < L_g$ or $\|\mathbf{g}_k\| > tolerance$ **then**
      return Error goal reached
    Compute the β with one of the methods HS, MHS, FR, PR
    Compute the direction: $\mathbf{d}_k \leftarrow -\mathbf{g}_k + \beta \mathbf{d}_k$
    Compute the learning rate α_k with a Line Search
    Update the weights: $\mathbf{W}_{k+1} \leftarrow \mathbf{W}_k + \alpha_k \mathbf{d}_k$
    $k \leftarrow k + 1$

2.2.1 Search Direction

The direction $\mathbf{d}_k$ holds the sequent property:

$$\mathbf{d}_k^T \mathbf{H} \mathbf{d}_{tk-1} = 0, \tag{2.13}$$

that means it is conjugate to the previous direction $\mathbf{d}_{k-1}$. Furthermore, it doesn't need to know all the previous directions, but it only needs the last one, which is why it requires very little storage and computation.
When dealing with quadratic functions, this method keeps the progress obtained so far in the minimization of the Loss function, by ensuring that the gradient along the previous direction does not increase. Anyway, it's worth to underline that this method can also be applyed with nonlinear functions: in this case, it should be necessary to restart the process, since there is no assumption that the conjugate directions previously found are still at the minimum of the function.
Each new direction it's a linear combination of the steepest descent -**g** and the previous direction $\mathbf{d}_{k-1}$, and it is defined as:

$$\mathbf{d}_k = \begin{cases} -\mathbf{g}_0, & \text{if } k = 0; \\ -\mathbf{g}_k + \beta_k \mathbf{d}_{k-1}, & \text{otherwise,} \end{cases} \tag{2.14}$$

where β_k is a scalar, to be determined, that says how much of the previous direction should be added to the newest one. When applied to minimize a strictly convex quadratic function, it ensure that the directions $\mathbf{d}_k$ and $\mathbf{d}_{k-1}$ are conjugate with respective to the Hessian of the objective function, that is the property 2.2.1 holds.
Of course, the first search direction when $k = 0$ is defined as the steepest descent direction at the initial weight $\mathbf{W}_0$ while, for $k > 1$, a minimization along each of the search direction is performed.
Since it may be that the direction found is not a descent direction of the objective function, another modified search direction, proposed by Zang et al.[12], has been tested in the project. It ensures sufficient descent $g_k^T = -\|g_k\|^2$, indipendent of the line search used or the convexity of the objective function, and is defined as follows:

$$\mathbf{d}_k^+ = \begin{cases} -\mathbf{g}_0, & \text{if } k = 0; \\ -(1 + \beta_k \frac{\mathbf{g}_k^T \mathbf{d}_k}{\|\mathbf{g}_k\|}) \mathbf{g}_k + \beta_k \mathbf{d}_{k-1}^+, & \text{otherwise.} \end{cases} \tag{2.15}$$

2.2.2 Beta

What really makes the difference in the computation of the conjugate gradient algorithm, is the choice of the method used to compute the β coefficient.
In fact, there has been proposed various choices for computing it, each one giving different efficiency and properties.
The formulas tested in our implementation are three: the Polak-Ribierère (PR), the Hestenes-Stiefel (HS) and a Modified Hestenes-Stiefel (MHS^+).
One of the properties that must be garanteed, is the global convergence of the method. When the function to be minimized is convex and quadratic, indeed, the Conjugate Gradient algorithm ensures the convergence and the detection of the global minimum in at most N iterations, that is the number of dimensions. Often, expecially when N is very large, there are great chances that the algorithm terminates in less than N epochs. [4]. However, since in our network we are dealing with a nonquadratic Loss function, as showed in §1.5.1, the direction computed as in Eq. 2.14 could not be a descent direction. In order to avoid this issue, all the methods have been modified as follows, ensuring the global convergence [6]:

$$\beta^+ = max\{\beta, 0\}. \tag{2.16}$$

This change provides a sort of restart of the algorithm, in case the β found is negative. This is equivalent to forget the last search direction and start again the search from the steepest descent direction. The use of β in Eq. 2.16 is similar to adopt the strategy of restarting the algorithm after N steps, initializing d_k to the current steepest descent direction [16, 7].

$$\beta_k^{PR} = \frac{\mathbf{g}_k^T(\mathbf{g}_k - \mathbf{g}_{k-1})}{\|\mathbf{g}_{k-1}\|^2},\ \beta_k^{HS} = \frac{\mathbf{g}_k^T(\mathbf{g}_k - \mathbf{g}_{k-1})}{(\mathbf{g}_k - \mathbf{g}_{k-1}^T\mathbf{d}_{k-1})}. \tag{2.17}$$

The HS and the PR methods in Eq. 2.17 have very similar performances and they are two of the most efficient conjugate gradient methods, but they are not globally convergent for nonlinear function[10]. That's why the modification of Eq. 2.16 has been adopted[18], since it enforces the descent property of the algorithm. Both the methods are formulated in such a way that, when occurring small steps, the search direction found is close to the negative gradient direction, getting a final step of decent size[7]. Moreover, the HS method is considered superior to other methods when applied to nonquadratic functions.
If we assume the Assumption 1 and we use a β HS or PR, modified as in Eq.2.16 and a Line Search as the one described in §2.2.3, then it holds the convergence of the algorithm as follows[7]:

$$\lim_{k\to\infty} \|\mathbf{g}_k\| = 0, \tag{2.18}$$

a weaker result with respect to the one involved with strongly convex functions, $\lim_{k\to\infty} \mathbf{g}_k = 0$.
The last method tested is the MHS^+, a modified version of the Hestenes-Stiefel one [13]. It garantees sufficient descent with inexact line search and is based on a modified secant equation which approximates the second order information of the Loss function with high order accuracy. Moreover, it is globally convergent.
It is defined as follows:

$$\beta_k^{MHS} = \frac{\mathbf{g}_k^T\widetilde{\mathbf{y}}_{k-1}^*}{\mathbf{d}_{k-1}^T\widetilde{\mathbf{y}}_{k-1}^*}. \tag{2.19}$$

In order to better understand the formula 2.19, it's important to describe all the components involved in its definiton.

When dealing with quasi-Newton methods, an approximation $\mathbf{B}_{k-1}$ of the Hessian of the Loss function $\nabla^2 L_{k-1}$ is update such that $\mathbf{B}_k$ satisfies the secant condition:

$$\mathbf{B}_k(\mathbf{W}_k - \mathbf{W}_{k-1}) = \mathbf{y}_{k-1}, \tag{2.20}$$

where $\mathbf{y}_{k-1}$ is defined as $\mathbf{g}_k - \mathbf{g}_{k-1}$.
Wei et al. [19] derived a class of modified secant condition:

$$\mathbf{B}_{k-1}(\mathbf{W}_k - \mathbf{W}_{k-1}) = \widetilde{\mathbf{y}}_{k-1}, \tag{2.21}$$

$$\widetilde{\mathbf{y}}_{k-1} = \mathbf{y}_{k-1} + \frac{\theta_{k-1}}{(\mathbf{W}_k - \mathbf{W}_{k-1})^T \mathbf{u}}\mathbf{u}, \tag{2.22}$$

with $\mathbf{u}$ a vector satisying $(\mathbf{W}_k - \mathbf{W}_{k-1})^T \mathbf{u} \neq 0$ and θ_{k-1} defined as:

$$\theta_{k-1} = 2(L_{k-1} - L_k) + (\mathbf{g}_k + \mathbf{g}_{k-1})^T (\mathbf{W}_k - \mathbf{W}_{k-1}). \tag{2.23}$$

Since for $\|(\mathbf{W}_k - \mathbf{W}_{k-1})\| > 1$ the standard secant Eq.2.20 better approximates $\nabla^2 L_{k-1}(\mathbf{W}_k - \mathbf{W}_{k-1})$ than the modified version in Eq.2.22, Livieris and Pintelas[13] proposed a modification of the equation in this way:

$$\mathbf{B}_{k-1}(\mathbf{W}_k - \mathbf{W}_{k-1}) = \widetilde{\mathbf{y}}^*_{k-1}, \tag{2.24}$$

$$\widetilde{\mathbf{y}}^*_{k-1} = \mathbf{y}_{k-1} + \rho_{k-1}\frac{max\{\theta_{k-1}, 0\}}{(\mathbf{W}_k - \mathbf{W}_{k-1})^T \mathbf{u}}\mathbf{u}, \tag{2.25}$$

where $\rho_{k-1} \in \{0, 1\}$ is a parameter that switch between the standard secant equation Eq.2.20 and the modified one Eq.2.24, setting ρ_{k-1} as:

$$\rho_{k-1} = \begin{cases} 1, & \text{if } \|(\mathbf{W}_k - \mathbf{W}_{k-1})\| \leq 1; \\ 0, & \text{otherwise.} \end{cases} \tag{2.26}$$

Since the following assumptions are satisfied by the Loss functions in Eq.1.5:

Assumption 3 - *The level set* $\mathcal{L} = \{w \in \mathbb{R}^n | L(\boldsymbol{W}) \leq L(\boldsymbol{W}_0)\}$ *is bounded, there exist a constant* $B > 0$ *s.t.* $\|\boldsymbol{W}\| \leq B, \forall \boldsymbol{W} \in \mathcal{L}$*;*

Assumption 4 - *If in some neighborhood* $\mathcal{N} \in \mathcal{L}$*, L is differentiable and its gradient* $\boldsymbol{g}$ *is Lipschitz continuous, then there exists a constant* $L > 0$ *such that*

$$\|\boldsymbol{g}(\boldsymbol{W}) - \boldsymbol{g}(\widetilde{\boldsymbol{W}})\| \leq L\|\boldsymbol{W} - \widetilde{\boldsymbol{W}}\|, \forall \ \boldsymbol{W}, \widetilde{\boldsymbol{W}} \in \mathcal{N}, \tag{2.27}$$

if the conjugate gradient algorithm is performed using MSH^+ and computing the search direction $\mathbf{d}^+$ as defined by Eq.2.15, we have:

$$\lim_{k\to\infty} \|\mathbf{g}_k\| = 0, \tag{2.28}$$

that is the convergence of the algorithm.
Assumption 3 is satisfied, since, as we have said before, our loss function is bounded in the interval $(0, 1)$, and hence the level set is also bounded. Assumption 4 is also satisfied, having described the properties for our loss function in section 1.5.

2.2.3 Line Search

Once computed the new direction $\mathbf{d}$ involved in the new weights $\mathbf{W}+\alpha\mathbf{d}$, a line search has to be implemented in order to find the right step size which minimize the Loss function.
The step size α is nothing more than a scalar: the learning rate for the conjugate gradient algorithm, which tells how far is right to move along a given direction.
So, fixed the values of the weights $\mathbf{W}$ and the descent direction $\mathbf{d}$, the main goal is to find the right value for α that is able to minimize the Loss function:

$$\min_{\alpha} \quad L(\mathbf{W} + \alpha\mathbf{d}). \tag{2.29}$$

Of course, we have to deal with a tradeoff: we want a good reduction, but we can't spend too much time computing the exact value for the optimum solution. So, the smarter way to get it is to use an inexact line search, that try some candidate step size and accepts the first one satisfying some conditions.
This search is performed in two phases:

- a *bracketing phase*, that finds an initial interval containing a minimizer;
- an *interpolation phase* that, given the interval, finds the right step length in it.

We decided to use one of the most popular line search condition: the *Armijo-Wolfe* condition.
The search for the better α is led by two condition:

- the *Armijo* one:
$$L(\mathbf{W}_k + \alpha_k\mathbf{d}_k) \leq L(\mathbf{W}_k) + \sigma_1\alpha\nabla L_k^T\mathbf{d}_k \tag{2.30}$$
which ensure that α gives a sufficient decrease of the objective function, being this reduction proportional to the step length α and the directional derivative $\nabla L_k^T d_k$.
The constant σ_1 has been set $\sigma_1 = 10^{-4}$, since it is suggested in literature to be quite small.

- the *Strong Wolfe* condition:
$$|\nabla L(\mathbf{W}_k + \alpha_k\mathbf{d}_k)^T\mathbf{d}_k| \leq L(\mathbf{W}_k) + \sigma_2|\nabla L_k^T\mathbf{d}_k| \tag{2.31}$$
which garantees to choose steps whose size is not too small.
It is also known as curvature condition and ensures that, moving of a step α along the given direction, the slope of our function if greater than σ_2 times the original gradient (if the slope is only slightly negative, the function cannot decrease rapidly along that direction, so it's better to stop the search).
In this case, the constant σ_2 is equal to 0.1, since a smaller value gives a more accurate line search. Futhermore, having choosen the strong condition, which doesn't allow the derivative to be too positive, we are sure that the α found lies close to a stationary point of the function.

The algorithm satisfing the Strong Wolfe conditions is implemented through the functions described in the pseudocodes 5, 6 and is based on the the algorithms presented in [3], chapter 3.
Since two consecutive values may be similar in finite-precision arithmetic, we set a threshold in both the `line_search` and the quadratic interpolation functions, which garantees that the algorithm stops if two values of α are too close or if the maximum number of iterations has been reached.

Algorithm 5 Line Search satisfying the strong Wolfe conditions. $\alpha_1 > 0$ and α_{max} are given.

procedure LINE_SEARCH
  $\alpha_0 \leftarrow 0$;
  $i \leftarrow 1$;
  while $i \leq max\_iter$ **do**
    Evaluate$L(\alpha_i)$;
    if $[L(\alpha_i) > L(0) + \sigma_1 \alpha_i \nabla L_0^T d_0]$ or $[L(\alpha_i) \leq L(\alpha_{i-1})$ and $i > 1]$ **then**
      $\alpha_* \leftarrow$ **zoom**(α_{i-1}, α_i); **return** α_*;
    Evaluate ∇L_i
    if $|\nabla L_i| \leq -\sigma_2 \nabla L_0^T d_0$ **then**
      $\alpha_* \leftarrow \alpha_i$; **return** α_*;
    if $\nabla L_i \geq 0$ **then**
      $\alpha_* \leftarrow$ **zoom**(α_i, α_{i-1}); **return** α_*;
    if $(|L_i - L_{i-1}| \leq threshold$ **then**
      $\alpha_* \leftarrow \alpha_i$ **return** α_*;
    Choose $\alpha_{i+1} \in (\alpha_i, \alpha_{max})$;
    $i \leftarrow i + 1$;

Algorithm 6 Zoom

procedure ZOOM
  while True **do**
    $\alpha_j \leftarrow quadratic\_interpolation(\alpha_{lo}, \alpha_{hi})$;
    Evaluate $L(\alpha_j)$;
    if $\left[L(\alpha_j) > L(0) + \sigma_1 \alpha_j \nabla L_0^T d_0\right]$ or $[L(\alpha_j) \leq L(\alpha_{lo})]$ **then**
      $\alpha_* \leftarrow \alpha_j$;
      return α_*;
    else
      Evaluate $\nabla L_j^T d_j$;
      if $\left|\nabla L_j^T d_j\right| \leq -\sigma_2 \nabla L_0^T d_0$ **then**
        $\alpha_* \leftarrow \alpha_j$;
        return α_*;
      if $\nabla L_j^T d_j (\alpha_{hi} - \alpha_{lo}) \geq 0$ **then**
        $\alpha_{hi} \leftarrow \alpha_{lo}$;
      if $(|L_j - L_0| \leq threshold$ **then**
        $\alpha_* \leftarrow \alpha_j$
        return α_*;
    $\alpha_{lo} \leftarrow \alpha_j$;

Chapter 3

Experiments

In this final chapter we present the results we obtained by applying our model to the datasets we have used to validate and test our ANN, namely, MONKS and CUP. Other than the results, we also present some details about the validation phase for each one of the datasets. In appendix A and B we added some graphs of the ANN's performances during the experimental phases, in order to enrich the presentation.

3.1 MONKS

Before delving into the details of the results we obtained by applying our model to the dataset, we provide some informations about the *preprocessing routines* and *validation schema* we decided to use. Here are the steps we followed in order to reach the final states of our analysis.

1. Since the MONKS datasets' feature are categorical, that is, every feature's value represents a class, not a numerical value, we preprocessed the three datasets by writing a script for applying a *1-of-k encoding*, hence obtaining 17 binary input features.

2. As a supplementary preprocessing phase, we have applied a *symmetrization* to the matrix containing the dataset's values, in order to ease the training during the validation phase by having a matrix of values closer to the symmetric behavior of the sigmoid function, which was introduced in section 1.4.

3. Since we have chosen to follow [1] for the hyperparameters' search during the validation phase, we first performed some *preliminary trials* in order to have a glimpse on the best intervals for searching our model's hyperparameters. During this trials we manually varied the model's hyperparameters, e.g. the learning rate, the momentum constant and so on for the SGD and the rho constant for the CGD, and observed the resulting *learning curves*. For this part of the analysis we have used the 20% of the training set as validation set, and the remaining part for training the network.

4. We then deepen the search using the most interesting intervals discovered during the preliminary trials in the validation phase by using our implementation of the (random) *grid search algorithm*, in which we also used our implementation of the *k-fold cross validation algorithm* (which follows the approach of using a value of 5 for the k parameter).

Our validation schema for the MONKS dataset essentially consists in using the random grid search algorithm to investigate some random sampled "points" in the hyperparameters' space, evaluating the performances for each one of this points and finally selecting the best

combinations of parameters based on the diffent metrics like *generalization error*, *accuracy*, *precision*, *recall* and *f1-score*. In Tab. 3.1 are reported the ranges for the hyperparameters involved in the validation phase.

Table 3.1: Hyperparameters' ranges for the random grid search algorithm with SGD and CG.

Hyperparameters	Ranges
η	$[0.6, 0.8]$
α	$[0.5, 0.9]$
λ	$[0.001, 0.01]$

Hyperparameters	Ranges
σ_2	$[0.1, 0.4]$
ρ	$[0.0, 1.0]$

In order to compare the results in a similar configuration between the SGD and the CG, we have decided to adopt only the *batch* mode for training the ANN.
In the following tables, the tasks are divided by the kind of dataset that has been used during the iteration, and, for each one of the tasks, the network's topology is the same, that is, 17 -> 4 -> 8 -> 1.
For each task, the results concerning the MSE and the accuracy are collected by taking the mean of the output of 10 different iterations. In gray we can see the best optimizer for each one of the tasks. We added some additional statistics regarding the execution times in milliseconds of the various iterations. As for the other table, the best optimizers for each of the tasks are colored in gray.

3.1.1 Results (no max epochs)

In order to compare the behaviour of the different algorithms with a focus on the optimization, the accuracy, in term of convergence goal of the norm of the gradient, has been set to 10^{-3}.
All the methods have been trained with the same hyperparameters, and the only stopping criteria that has been chosen is the decreasing of the norm.

Task	Optimizer	σ_1	σ_2	ρ	η	α	λ	MSE (TR - TS)	Accuracy (TR - TS) (%)
MONK 1	SGD (CM)	-	-	-	0.61	0.83	0.0	1.00e-05 - 9.64e-06	100 % - 100 %
MONK 1	SGD (NAG)	-	-	-	0.61	0.83	0.0	1.39e-05 - 1.28e-05	100 % - 100 %
MONK 1	CGD (PR)	0.0001	0.3	0.0	-	-	-	6.11e-03 - 2.00e-02	99 % - 96 %
MONK 1	CGD (HS)	0.0001	0.3	0.0	-	-	-	6.11e-03 - 2.00e-02	99 % - 96 %
MONK 1	CGD (MHS)	0.0001	0.3	0.67	-	-	-	1.49e-05 - 1.43e-05	100 % - 100 %
MONK 2	SGD (CM)	-	-	-	0.61	0.83	0.0	7.56e-06 - 7.37e-06	100 % - 100 %
MONK 2	SGD (NAG)	-	-	-	0.61	0.83	0.0	9.27e-06 - 9.82e-06	100 % - 100 %
MONK 2	CGD (PR)	0.0001	0.3	0.0	-	-	-	8.41e-06 - 5.97e-06	100 % - 100 %
MONK 2	CGD (HS)	0.0001	0.3	0.0	-	-	-	8.38e-06 - 6.33e-06	100 % - 100 %
MONK 2	CGD (MHS)	0.0001	0.3	0.67	-	-	-	5.91e-06 - 5.72e-06	100 % - 100 %
MONK 3	SGD (CM)	-	-	-	0.61	0.83	0.0	2.07e-03 - 3.87e-06	97 % - 100 %
MONK 3	SGD (NAG)	-	-	-	0.61	0.83	0.0	1.78e-06 - 2.40e-06	100 % - 100 %
MONK 3	CGD (PR)	0.0001	0.3	0.0	-	-	-	1.43e-06 - 1.50e-06	100 % - 100 %
MONK 3	CGD (HS)	0.0001	0.3	0.0	-	-	-	6.20e-03 - 1.43e-06	99 % - 100 %
MONK 3	CGD (MHS)	0.0001	0.3	0.67	-	-	-	1.24e-02 - 3.80e-06	98 % - 100 %

Table 3.2: Comparisons between the iterations having no maximal number of epochs. Each one of the iterations has been completed with a network having topology 17 -> 4 -> 8 -> 1.

Task	Optimizer	Convergence Epoch	Elapsed Time	LS Iterations	BP Time	LS Time	Dir Time
MONK 1	SGD (CM)	25829	80835.78	-	6097.73	-	-
MONK 1	SGD (NAG)	14382	44410.24	-	3271.03	-	-
MONK 1	CGD (PR)	806	9728.46	8.0	1364.61	5750.07	15.10
MONK 1	CGD (HS)	770	9468.09	8.0	1324.35	5595.54	14.52
MONK 1	CGD (MHS)	472	5307.14	8.0	749.90	3151.04	7.26
MONK 2	SGD (CM)	14586	56437.37	-	3906.62	-	-
MONK 2	SGD (NAG)	7743	28037.07	-	1887.81	-	-
MONK 2	CGD (PR)	292	3944.34	8.0	579.52	2236.75	5.01
MONK 2	CGD (HS)	340	4385.45	8.0	650.30	2479.65	5.45
MONK 2	CGD (MHS)	513	6567.70	8.0	967.88	3769.13	8.12
MONK 3	SGD (CM)	65306	175429.15	-	13298.60	-	-
MONK 3	SGD (NAG)	50918	163439.49	-	12167.22	-	-
MONK 3	CGD (PR)	6540	74283.88	8.0	10581.14	44239.27	109.15
MONK 3	CGD (HS)	4056	50295.56	8.0	7223.92	29842.22	75.06
MONK 3	CGD (MHS)	2209	23903.49	8.0	3417.29	14174.89	32.84

Table 3.3: Additional time-related statistics. The unit of time that has been used is the millisecond.

In Table 3.2 and 3.3 we can find the results for the iterations completed without constraining the optimizers by imposing a maximal number of epochs of training.
It's immediately evident the different number of iterations that the Conjugate Gradient methods and the Stochastic Gradient Descent need in order to converge to the imposed threshold.
As we can expect from the theory, the CG methods are usually able to converge in the first 1000 iterations, while the SGD is extremely slower, needing more than 20000 iterations in order to arrive to the same level of accuracy.
It's worth to notice that the all these methods have to face some limitations when dealing with a noisy dataset as Monks 3, even though each one of them still confirms their typical behaviour.
Even when looking at the time of execution of the various algorithms, there is no surprise in the results. What is more interesting to underline is, as evident in the plots of Fig. 3.1, is the longer time needed by the SGD, even if a better performace is given by the use of the NAG momentum. When comparing the plots, we can see that, even though the number of iterations of the CG methods is different, when taking into account the time of execution, some iterations are more costly than other. That means, some methods could need more time in computing the right weights updates, even if they could converge in a lower number of iterations.
Futhermore, the majority of the time (more than half of the time) is spent in computing the Line Search, which tipically needs to perform 8 iterations in order to find the right learning step.
Taking into account also the accuracy in the prediction of the neural network, the MHS^{+} methods is the one having an overall better behaviour.

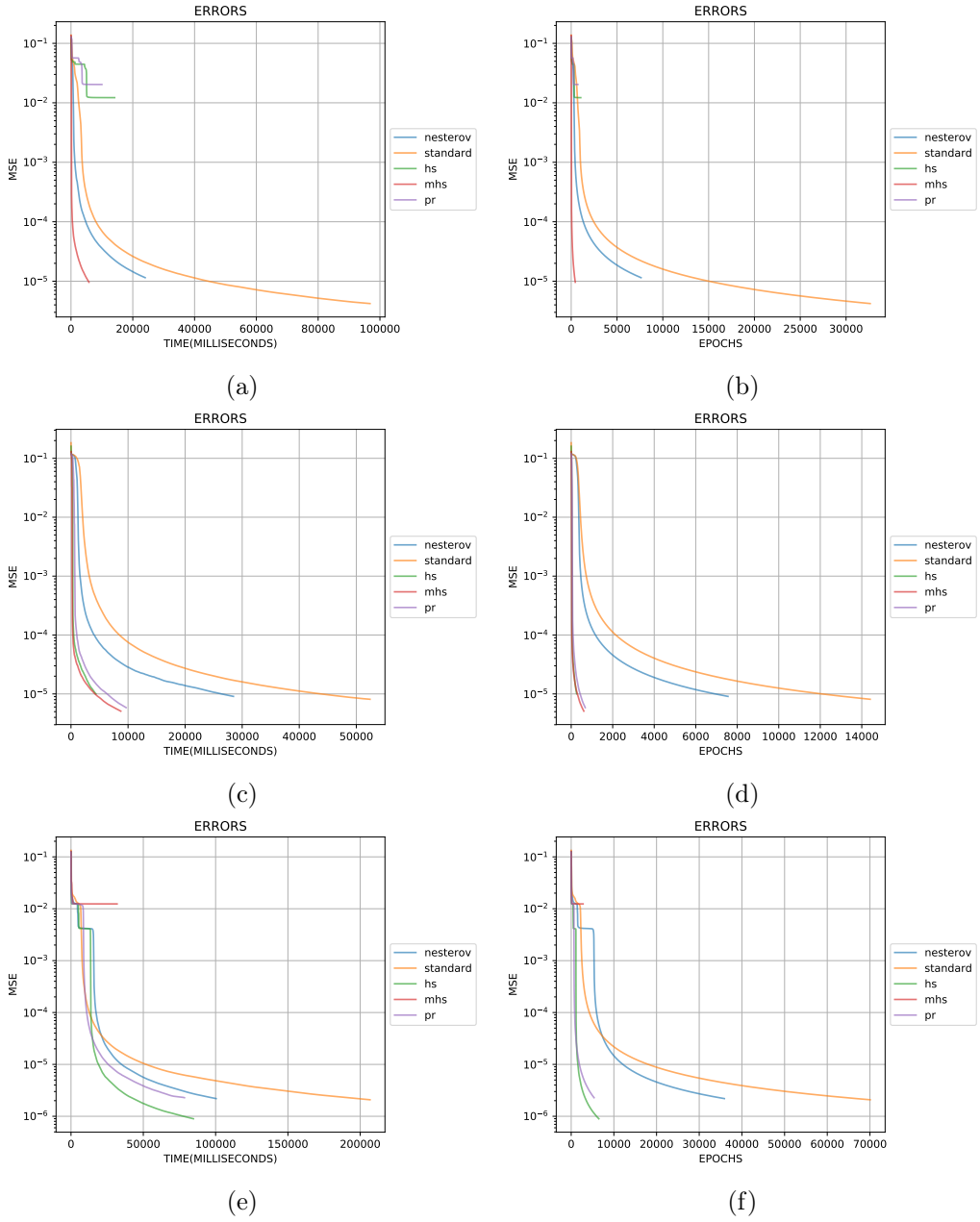

Figure 3.1: Comparisons between the different optimizers without the constrain of setting a maximal number of epochs for the iterations. In Figure A.1b, A.1a we can see the comparison for MONKS 1, while in Figure A.1d, A.1c we can see the one for MONKS 2 and finally in Figure A.1f, A.1e we can see the one for MONKS 3.

3.1.2 Results (max epochs 1000)

Task	Optimizer	σ_1	σ_2	ρ	η	α	λ	MSE (TR - TS)	Accuracy (TR - TS) (%)
MONK 1	SGD (CM)	-	-	-	0.65	0.75	0.0	9.92e-03 - 1.48e-02	99 % - 99 %
MONK 1	SGD (NAG)	-	-	-	0.63	0.73	0.0	2.18e-02 - 3.17e-02	97 % - 96 %
MONK 1	CGD (PR)	0.0001	0.18	0.0	-	-	-	1.54e-02 - 4.88e-02	97 % - 90 %
MONK 1	CGD (HS)	0.0001	0.22	0.0	-	-	-	2.12e-03 - 9.71e-03	100 % - 98 %
MONK 1	CGD (MHS)	0.0001	0.13	0.86	-	-	-	8.97e-03 - 1.92e-02	98 % - 96 %
MONK 2	SGD (CM)	-	-	-	0.71	0.89	0.0	6.99e-03 - 9.65e-03	100 % - 100 %
MONK 2	SGD (NAG)	-	-	-	0.64	0.85	0.0	1.34e-02 - 1.91e-02	98 % - 98 %
MONK 2	CGD (PR)	0.0001	0.34	0.0	-	-	-	1.59e-02 - 3.86e-02	96 % - 92 %
MONK 2	CGD (HS)	0.0001	0.17	0.0	-	-	-	1.06e-02 - 1.43e-02	98 % - 97 %
MONK 2	CGD (MHS)	0.0001	0.33	0.43	-	-	-	4.53e-03 - 1.13e-02	99 % - 98 %
MONK 3	SGD (CM)	-	-	-	0.67	0.85	0.0027	1.18e-02 - 1.31e-02	98 % - 98 %
MONK 3	SGD (NAG)	-	-	-	0.61	0.80	0.0036	1.67e-02 - 1.98e-02	97 % - 97 %
MONK 3	CGD (PR)	0.0001	0.19	0.0	-	-	-	2.07e-02 - 3.51e-02	94 % - 93 %
MONK 3	CGD (HS)	0.0001	0.36	0.0	-	-	-	9.03e-03 - 1.95e-02	98 % - 96 %
MONK 3	CGD (MHS)	0.0001	0.34	0.42	-	-	-	7.01e-03 - 1.63e-02	99 % - 96 %

Table 3.4: Comparisons between the iterations having a maximal number of epochs egual to 1000. Each one of the iterations has been completed with a network having topology 17 -> 4 -> 8 -> 1.

Task	Optimizer	Convergence Epoch	Elapsed Time	LS Iterations	BP Time	LS Time	Dir Time
MONK 1	SGD (CM)	1000	5163.25	-	149.95	-	-
MONK 1	SGD (NAG)	1000	5214.20	-	147.68	-	-
MONK 1	CGD (PR)	445	5055.85	6.0	514.70	2233.17	14.00
MONK 1	CGD (HS)	240	2665.58	6.0	267.58	1164.87	7.95
MONK 1	CGD (MHS)	298	3278.08	7.0	328.36	1436.53	9.57
MONK 2	SGD (CM)	1000	5385.27	-	159.47	-	-
MONK 2	SGD (NAG)	1000	5437.32	-	157.63	-	-
MONK 2	CGD (PR)	326	3648.71	5.0	362.99	1603.26	10.17
MONK 2	CGD (HS)	149	1695.45	5.0	169.52	760.82	4.90
MONK 2	CGD (MHS)	183	2023.54	5.0	198.10	892.13	5.83
MONK 3	SGD (CM)	1000	5304.07	-	155.96	-	-
MONK 3	SGD (NAG)	1000	5353.35	-	154.01	-	-
MONK 3	CGD (PR)	371	4149.39	5.0	418.39	1821.40	11.66
MONK 3	CGD (HS)	377	4319.66	6.0	439.25	1891.85	12.75
MONK 3	CGD (MHS)	389	4361.18	6.0	438.78	1906.62	12.70

Table 3.5: Additional time-related statistics. The unit of time that has been used is the millisecond.

Here we present the results from a series of iterations where the maximal number of epochs has been setted to 1000, in order to focus on a machine learning point of view. This time, the algorithms have been trained taking into account only the maximal number of epochs or the error goal=10^{-4} for the CG methods.
Similarly to the previous section, in Table 3.4 we can find the details regarding the optimizers' performances, while in Table 3.5 there are the details regarding the time-related performances. The considerations done for the iterations with no maximal number of epochs are valid also for this specific case. In Figure A.2 we can see a comparison betweeen the various optimizers.
In this case, it's more evident a behaviour introduced in the former experiments: in Monk 3, the CG methods and the SGD have spent a similar time of execution, even though the CG ones stopped in the first 300 iterations.
For what concernes the accuracy in the prediction, only few of the models get an accuracy of 100%, but it is still true that the CG gets very good results in a minor time of execution and in a minor number of iterations.

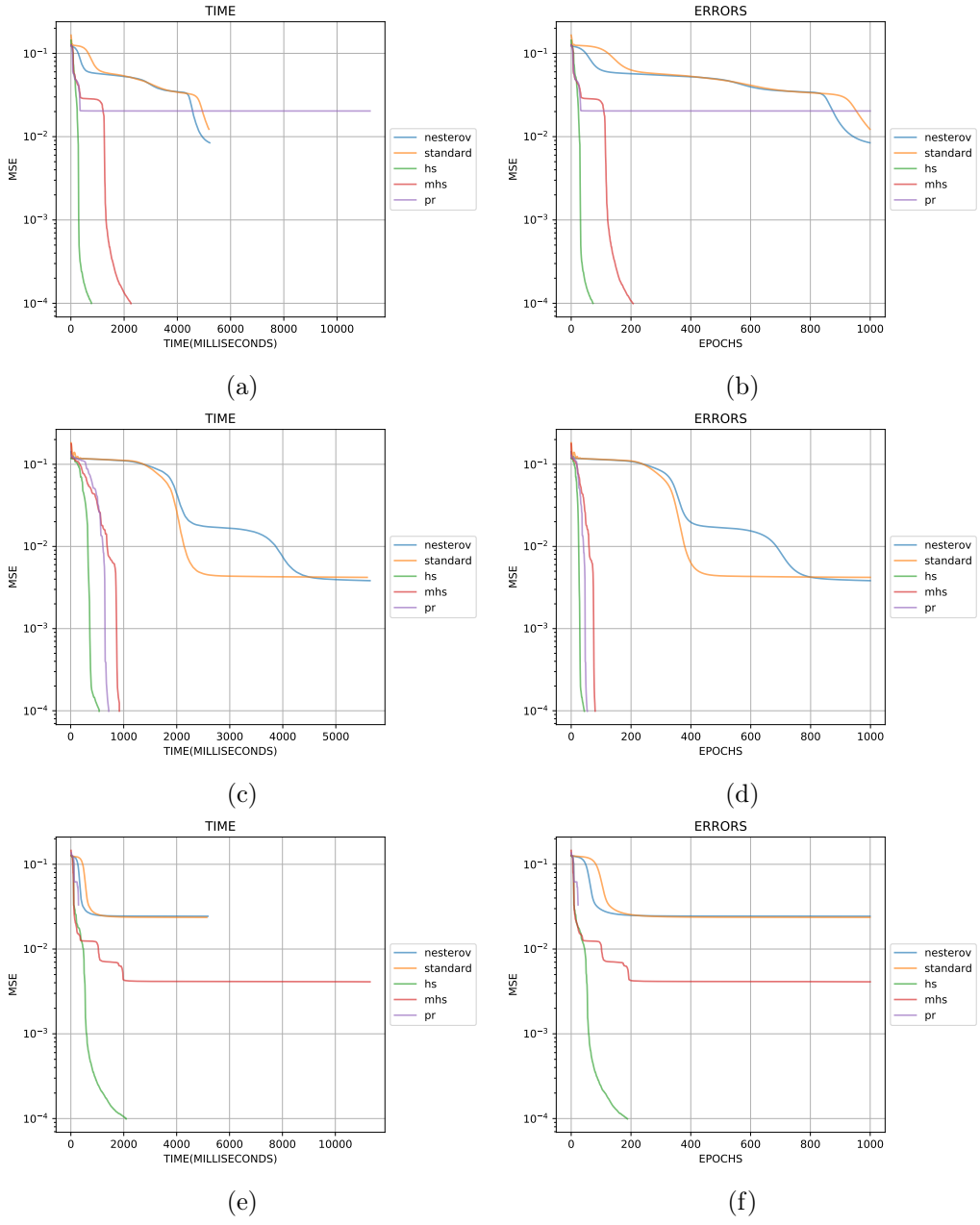

Figure 3.2: Comparisons between the different optimizers with the constrain of setting a maximal number of epochs egual to 1000. In Figure A.2b, A.2a we can see the comparison for MONKS 1, while in Figure A.2d, A.2c we can see the one for MONKS 2 and finally in Figure A.2f, A.2e we can see the one for MONKS 3.

3.2 CUP

A main difference with respect to the models used for Monk, is the choice of the topology of the Network. First of all, in this case, being the final task a regression one in which there are two different values to be predicted, the output layer of the ANN is composed by two neurons of output, each one associated to an identity function.
Then, after some preliminary trials, we have decided to set the number of the hidden layers to [16, 32].
Of course, as for the Monk dataset, we have performed a validation phase on the CUP dataset, in order to discover the best parameters for the network. As described in Sec. 3.1,

it has been implemented a *3-fold cross validation algorithm* with a (random) *grid search*. Table 3.6 shows the ranges in which the searching of the hyperparameters has been carried out. Once again, the momentum type chosen is Nesterov, while the direction used in the Conjugate Gradient Methods is the modified one.

Table 3.6: Hyperparameters' ranges for the random grid search algorithm with SGD and CG.

Hyperparameters	Ranges
η	$[0.004, 0.2]$
α	$[0.5, 0.9]$
λ	$[0.0003, 0.003]$

Hyperparameters	Ranges
σ_2	$[0.1, 0.4]$
ρ	$[0.0, 1.0]$

In tables 3.7 and 3.8 are annotated the average results obtained from 10 executions of each one of the best models identified thanks to the validation step.

Model	Topology	Batch size	Activation	η	α	λ	MSE (TR - TS)
SGD	10 -> 16 -> 32 -> 2	batch	identity	0.084	0.79	0.0009	1.00 - 1.35

Table 3.7: Results for the Stochastic Gradient Descent.

β	Topology	Batch size	Activation	σ_1	σ_2	ρ	MSE (TR - TS)
MHS^+	10 -> -> 16 -> 32 -> 2	batch	identity	0.0001	0.27	0.29	0.97 - 1.50
HS^+	10 ->-> 16 -> 32 -> 2	batch	identity	0.0001	0.39	0.0	0.97 - 1.50
PR^+	10 ->-> 16 -> 32 -> 2	batch	identity	0.0001	0.86	0.00	1.15 - 1.41

Table 3.8: Results for the Conjugate Gradient Methods.

As for the experiments with the Monk datasets, we attach the learning curves in Appendix B.

Appendix A

MONKS' learning curves

Here we present the *learning curves* for the three MONKS datasets. We have sampled these curves during the final tests on each dataset by plotting one of the 10 trails we used for building the statistics we presented in section 3.1, hence each plot presents a possible learning curve for the best hyperparameters' selection for each dataset. Alongside of the learning curves we also provide the *accuracy plots* in order to show how the accuracy score progresses during the epochs, and the *gradient's norm plots* in order to show the convergence rate. In the first sections we attach some plots in order to show the differences between the various models and to better compare their behaviour. Again, the plot are relative to one sampled execution between the 10 trails done.
The accuracy results are relative to the test set, while the norm and the error ones are relative to the training set.

A.1 Comparisons

A.1.1 No Max Epochs

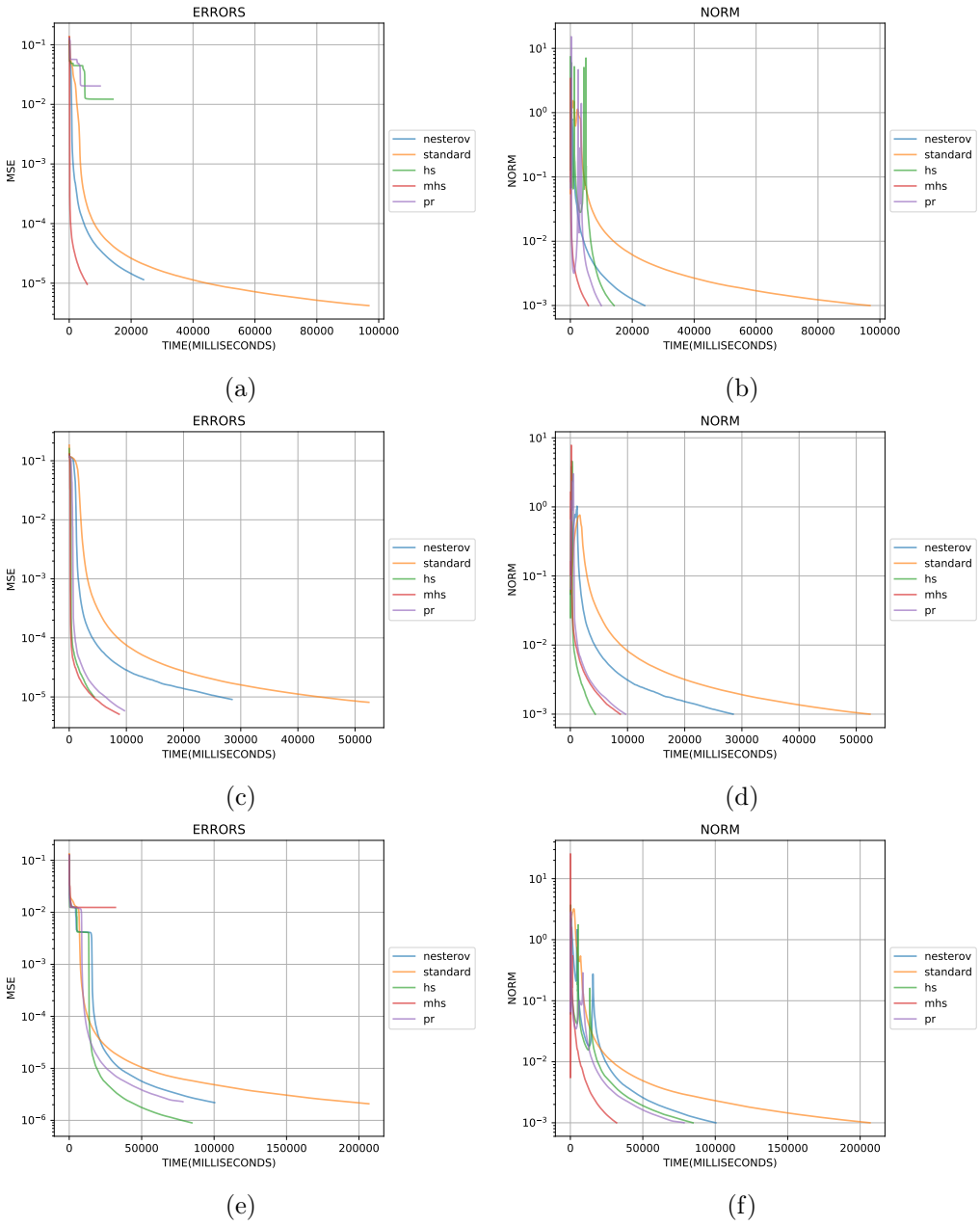

Figure A.1: Comparisons between convergence norm and error of the different optimizers without the constrain of setting a maximal number of epochs for the iterations. In Figure A.1b, A.1a we can see the comparison for MONKS 1, while in Figure A.1d, A.1c we can see the one for MONKS 2 and finally in Figure A.1f, A.1e we can see the one for MONKS 3.

A.1.2 Max Epochs 1000

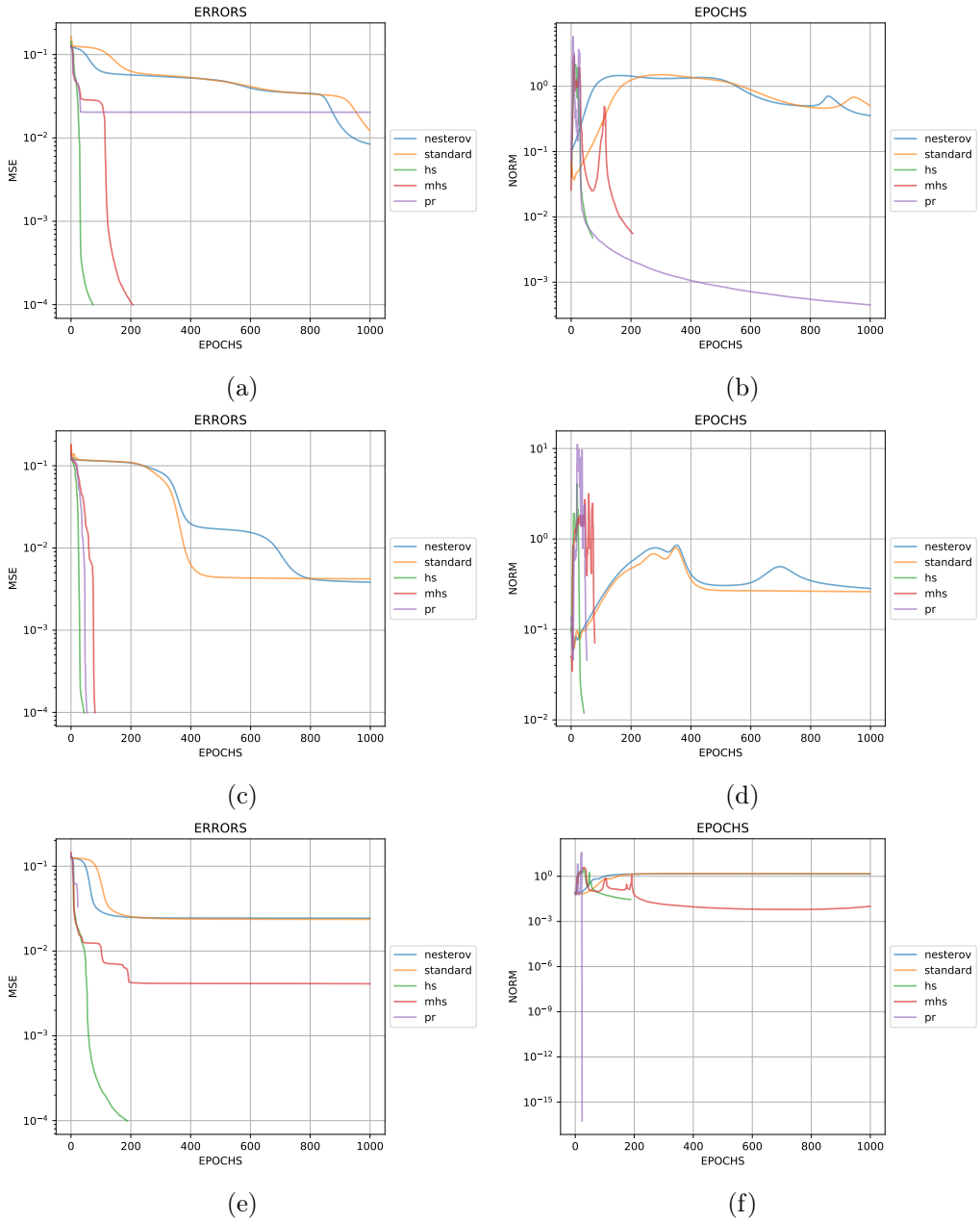

Figure A.2: Comparisons between convergence norm and error the different optimizers with the constrain of setting a maximal number of epochs egual to 1000. In Figure A.2b, A.2a we can see the comparison for MONKS 1, while in Figure A.2d, A.2c we can see the one for MONKS 2 and finally in Figure A.2f, A.2e we can see the one for MONKS 3.

A.2 Stochastic Gradient Descent

A.2.1 No Max Epochs

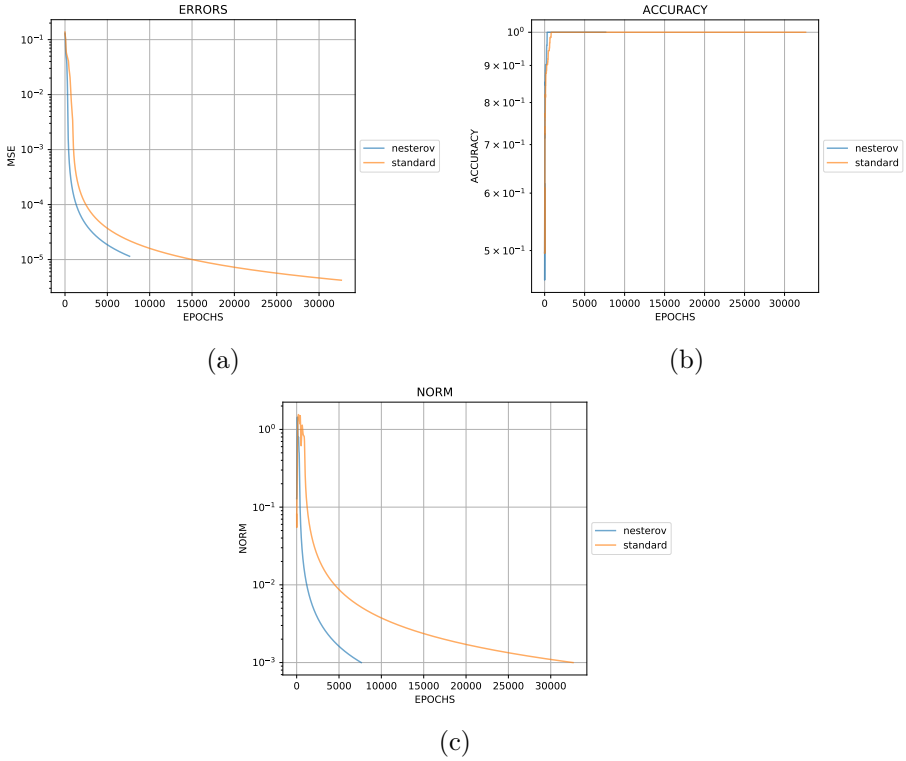

(a) (b)

(c)

Figure A.3: Example of a final learning, accuracy score and convergence of norm curve on MONKS 1 with standard and nesterov momentum.

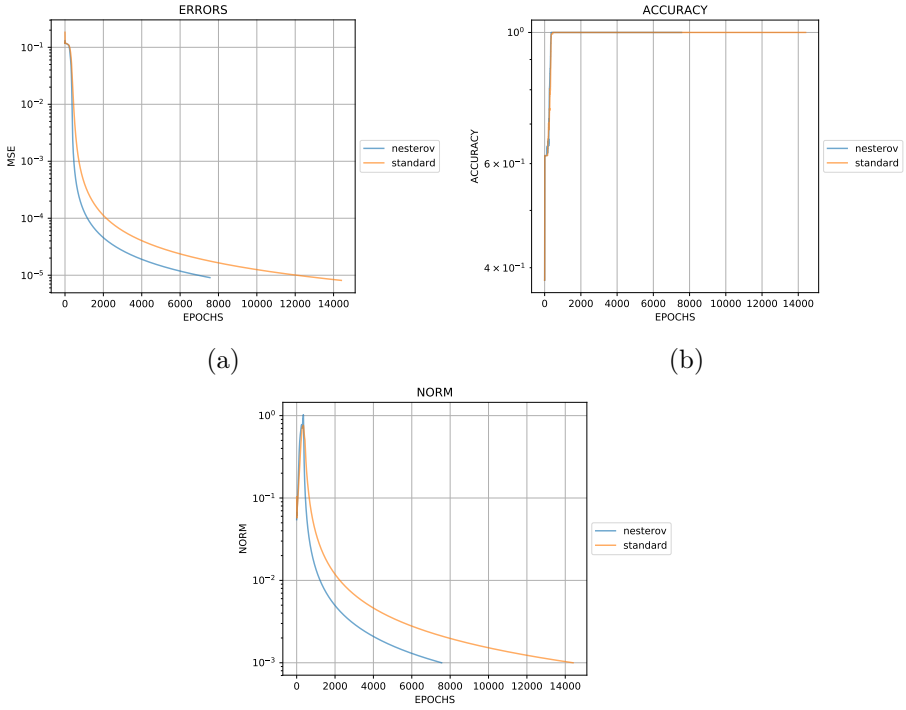

(a) (b)

(c)

Figure A.4: Example of a final learning, accuracy score and convergence of norm curve on MONKS 2 with standard and nesterov momentum.

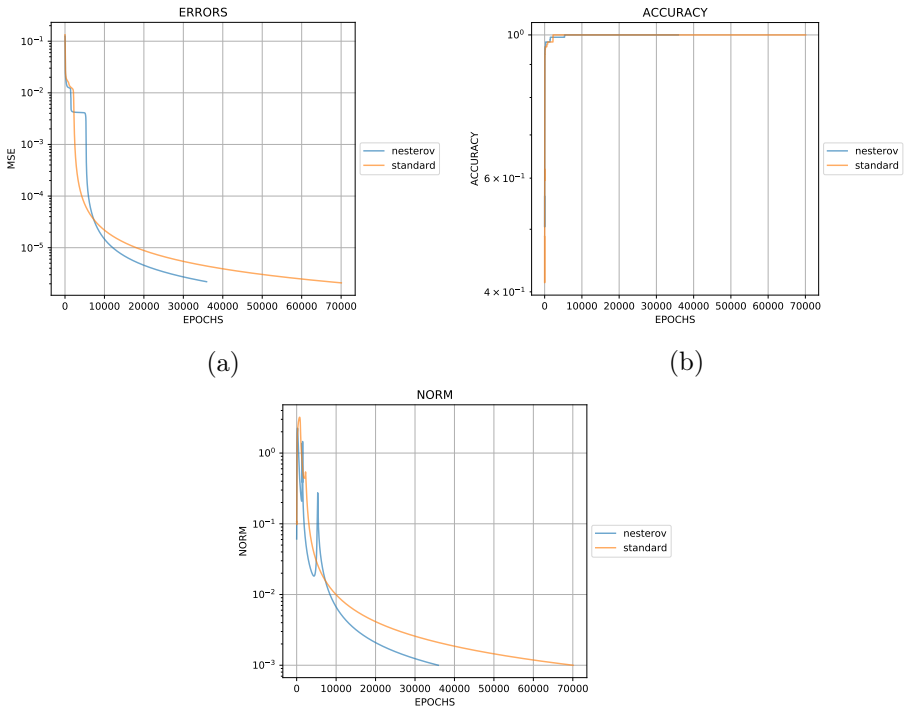

(a) (b)

(c)

Figure A.5: Example of a final learning, accuracy score and convergence of norm curve on MONKS 3 with standard and nesterov momentum.

A.2.2 Max Epochs 1000

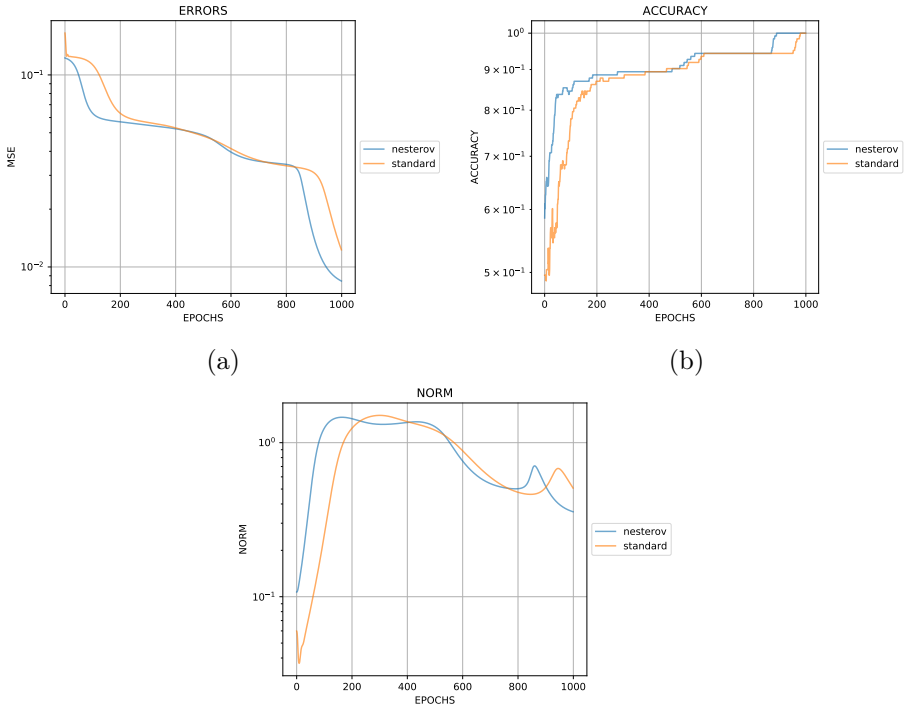

(a) (b)

(c)

Figure A.6: Example of a final learning, accuracy score and convergence of norm curve on MONKS 1 with standard and nesterov momentum.

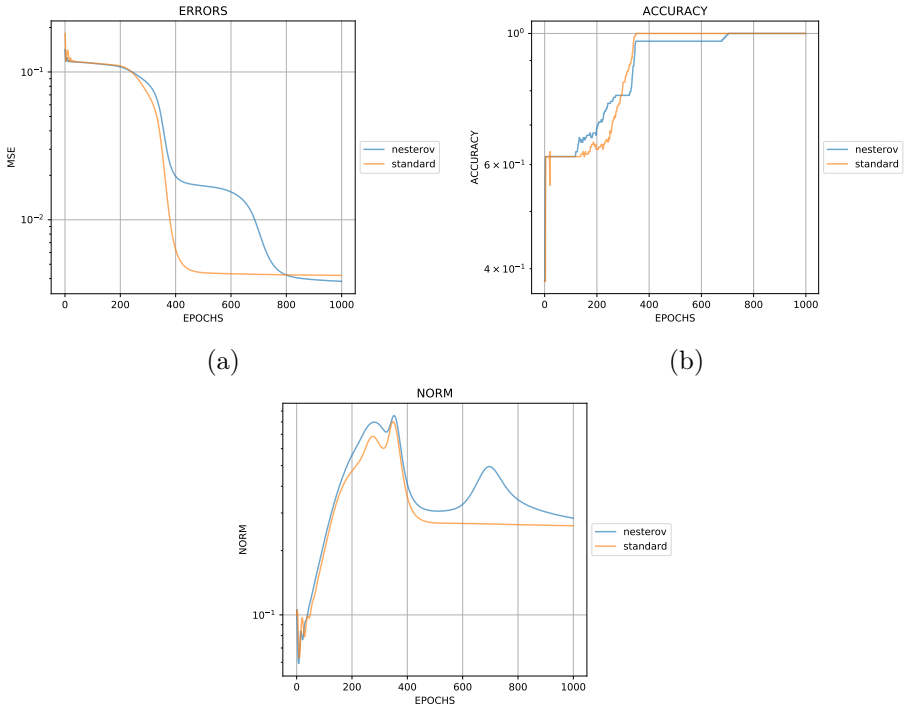

(a) (b)

(c)

Figure A.7: Example of a final learning, accuracy score and convergence of norm curve on MONKS 2 with standard and nesterov momentum.

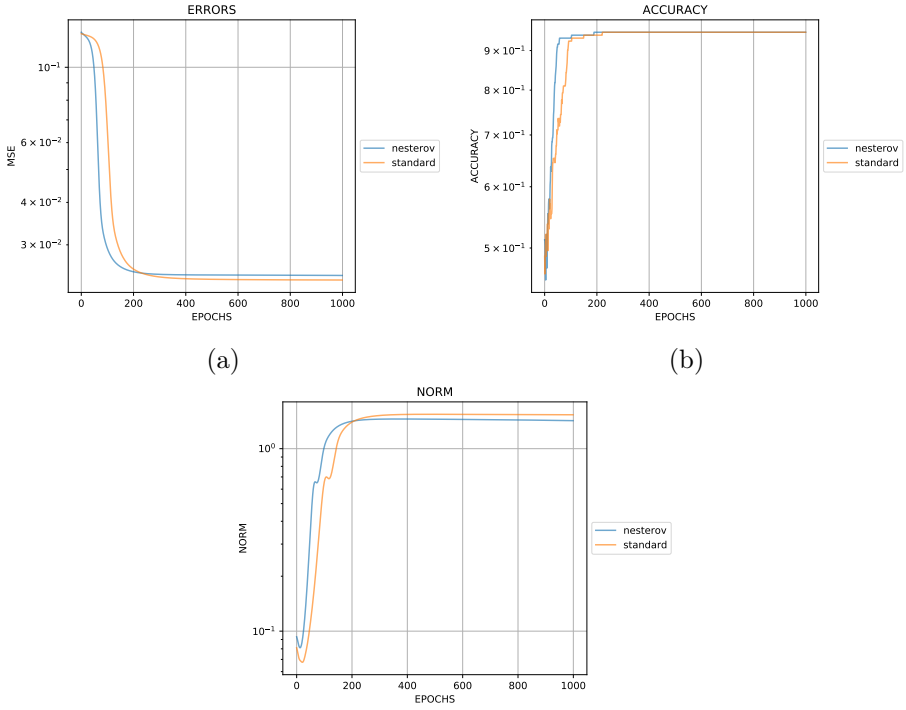

(a) (b)

(c)

Figure A.8: Example of a final learning, accuracy score and convergence of norm curve on MONKS 3 with standard and nesterov momentum.

A.3 Conjugate Gradient Methods

A.3.1 No Max Epochs

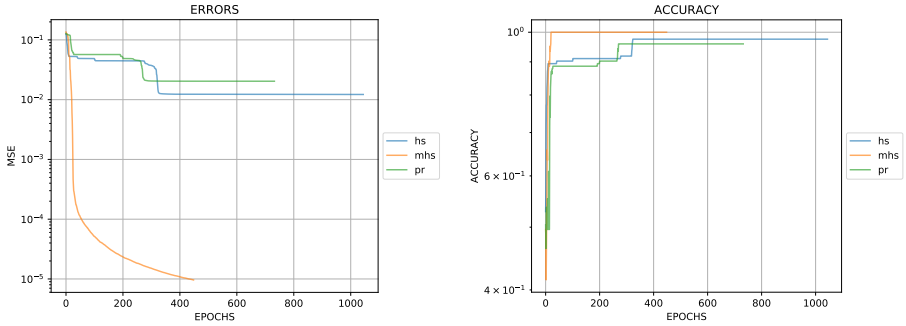

(a)

(b)

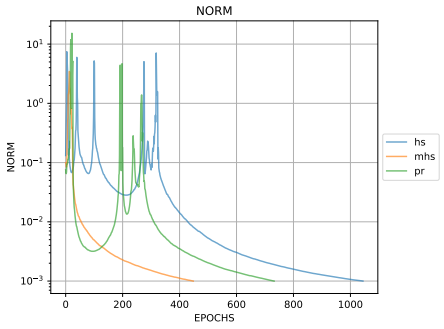

(c)

Figure A.9: Example of a final learning, accuracy score and convergence of norm curve on MONKS 1 with different beta methods.

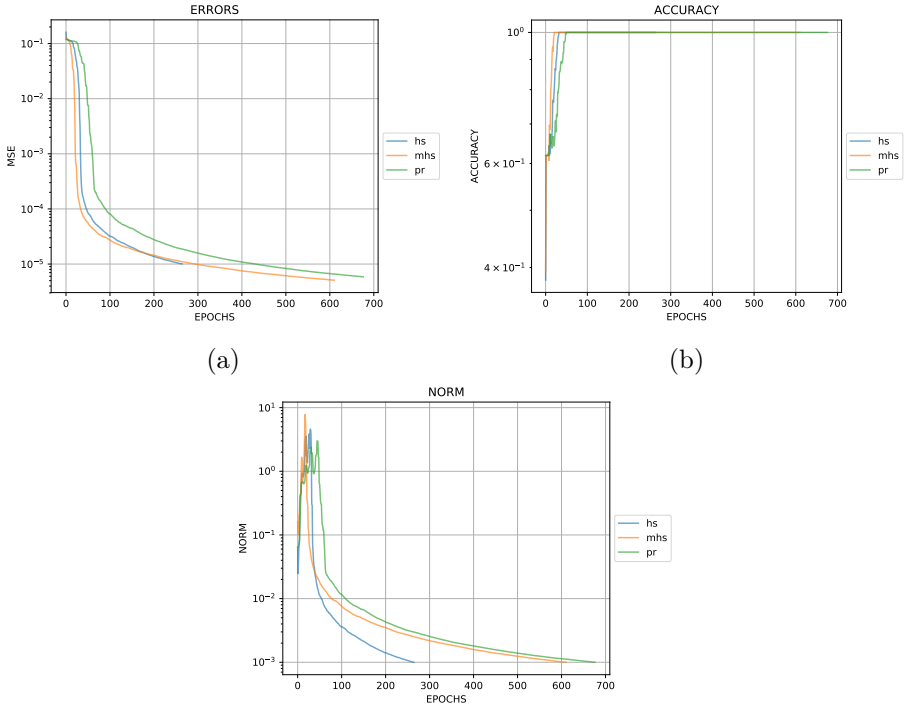

Figure A.10: Example of a final learning, accuracy score and convergence of norm curve on MONKS 2 with different beta methods.

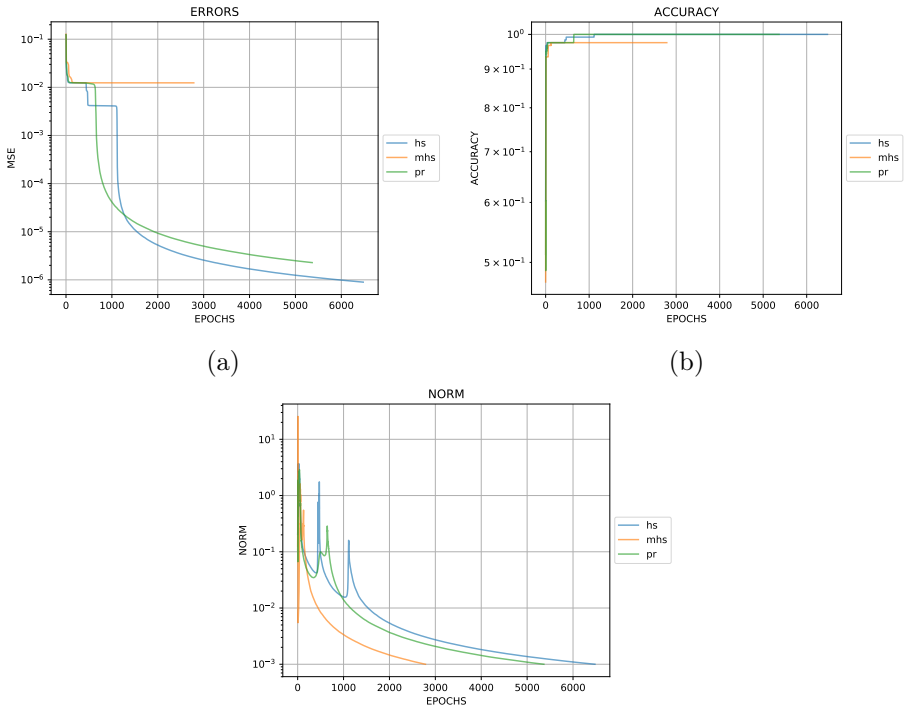

Figure A.11: Example of a final learning, accuracy score and convergence of norm curve on MONKS 3 with different beta methods.

A.3.2 Max Epochs 1000

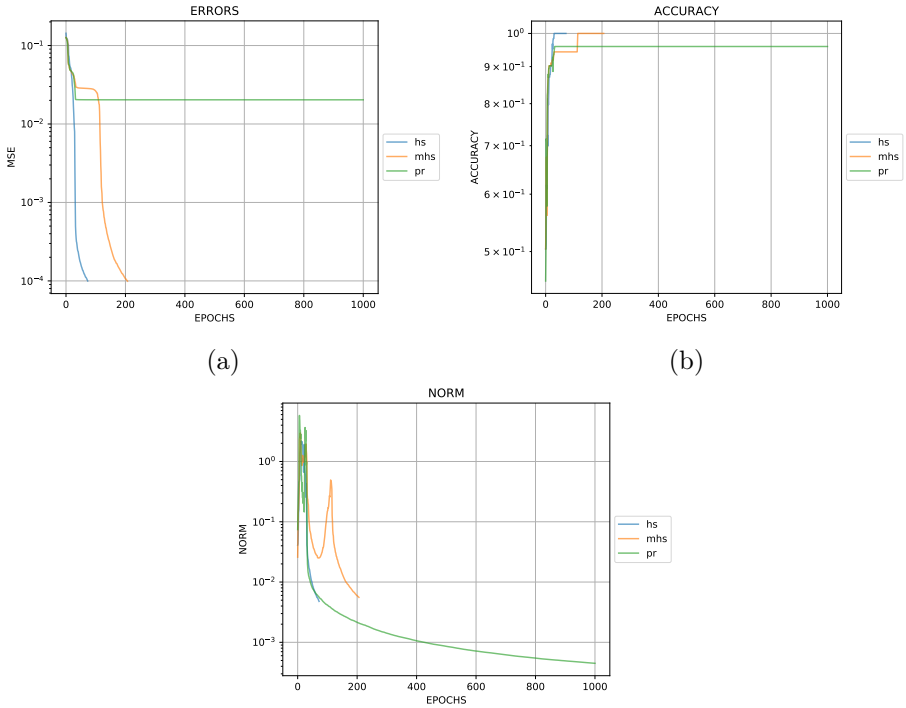

(a) (b)

(c)

Figure A.12: Example of a final learning, accuracy score and convergence of norm curve on MONKS 1 with different beta methods.

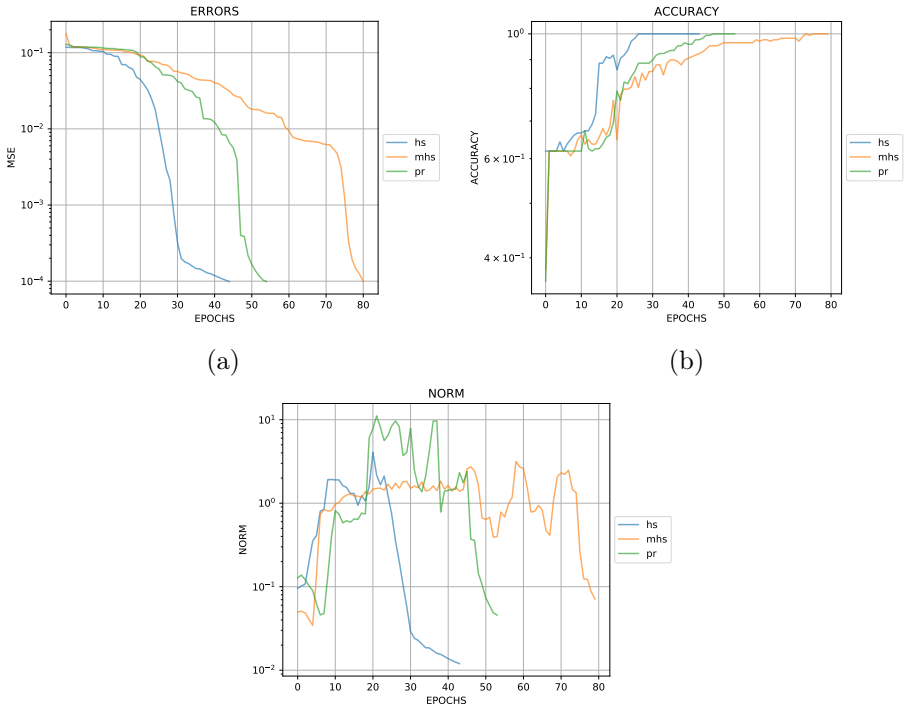

(a) (b)

(c)

Figure A.13: Example of a final learning, accuracy score and convergence of norm curve on MONKS 2 with different beta methods.

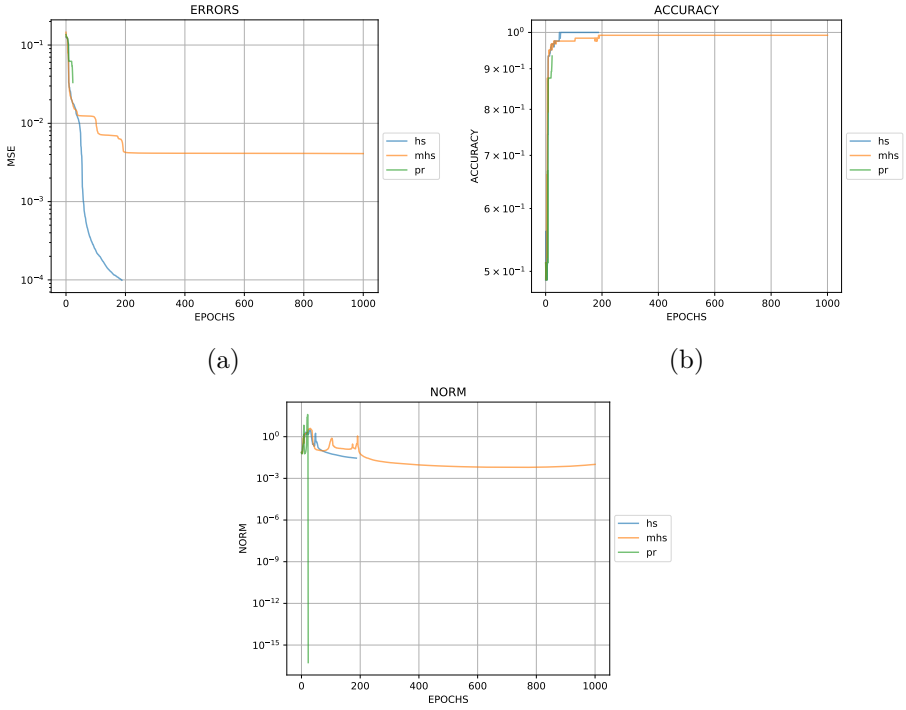

Figure A.14: Example of a final learning, accuracy score and convergence of norm curve on MONKS 3 with different beta methods.

Appendix B

CUP's learning curves

As in the previous section, the following curves are the result of the final tests on the test dataset. It has been plotted one of the 10 trails we used for building the statistics we presented in Section 3.2, hence each plot presents a possible learning curve for the best hyperparameters' selection for each dataset.

B.1 Stochastic Gradient Descent

Bibliography

[1] James Bergstra and Yoshua Bengio. Random search for hyper-parameter optimization. *J. Mach. Learn. Res.*, 13:281–305, 2 2012.

[2] Léon Bottou, Frank E. Curtis, and Jorge Nocedal. Optimization methods for large-scale machine learning, 2016. quantization overview.

[3] Stephen Boyd and Lieven Vandenberghe. *Convex Optimization*. Cambridge University Press, New York, NY, USA, 2004.

[4] L. C. W. DIXON. Conjugate gradient algorithms: Quadratic termination without linear searches. *IMA Journal of Applied Mathematics*, 15, 1975.

[5] Dheeru Dua and Casey Graff. UCI machine learning repository, 2017.

[6] J. Gilbert and J. Nocedal. Global convergence properties of conjugate gradient methods for optimization. *SIAM Journal on Optimization*, 2(1):21–42, 1992.

[7] Jorge Gilbert, Jean Charles; Nocedal. Global convergence properties of conjugate gradient methods for optimization. *SIAM Journal on Optimization*, 2, 02 1992.

[8] Xavier Glorot and Yoshua Bengio. Understanding the difficulty of training deep feedforward neural networks. In *In Proceedings of the International Conference on Artificial Intelligence and Statistics (AISTATS'10). Society for Artificial Intelligence and Statistics*, 2010.

[9] Ian Goodfellow, Yoshua Bengio, and Aaron Courville. *Deep Learning*. MIT Press, 2016. `http://www.deeplearningbook.org`.

[10] David F. Griffiths. *[Lecture Notes in Mathematics] Numerical Analysis Volume 1066 // Nonconvex minimization calculations and the conjugate gradient method*, volume 10.1007/BFb0099514. 1984.

[11] S.S. Haykin. *Neural Networks and Learning Machines*. Pearson International Edition. Pearson, 2009.

[12] Li Zhang; Weijun Zhou; Donghui Li. Global convergence of a modified fletcher-reeves conjugate gradient method with armijo-type line search. *Numerische Mathematik*, 104, 10 2006.

[13] Ioannis E. Livieris and Panagiotis Pintelas. A new conjugate gradient algorithm for training neural networks based on a modified secant equation. *Applied Mathematics and Computation*, 221:491 – 502, 2013.

[14] T.M. Mitchell. *Machine Learning*. McGraw-Hill International Editions. McGraw-Hill, 1997.

[15] Grgoire Montavon, Genevive Orr, and Klaus-Robert Mller. *Neural Networks: Tricks of the Trade*. Springer Publishing Company, Incorporated, 2nd edition, 2012.

[16] Martin Fodslette Møller. A scaled conjugate gradient algorithm for fast supervised learning. *Neural Networks*, 6(4):525 – 533, 1993.

[17] Y. E. NESTEROV. A method for solving the convex programming problem with convergence rate $o(1/k^2)$. *Dokl. Akad. Nauk SSSR*, 269:543–547, 1983.

[18] M J. D. Powell. Convergence properties of algorithms for nonlinear optimization. *SIAM Review*, 28, 12 1986.

[19] Zengxin Wei; Guoyin Li; Liqun Qi. New quasi-newton methods for unconstrained optimization problems. *Applied Mathematics and Computation*, 175, 2006.

[20] D. E. RUMERLHAR. Learning representation by back-propagating errors. *Nature*, 323:533–536, 1986.

[21] David Saad, editor. *On-line Learning in Neural Networks*. Cambridge University Press, New York, NY, USA, 1998.

[22] Shai Shalev-Shwartz and Ambuj Tewari. Stochastic methods for l1-regularized loss minimization. *Journal of Machine Learning Research*, 12:1865–1892, 2011.

[23] Ilya Sutskever, James Martens, George Dahl, and Geoffrey Hinton. On the importance of initialization and momentum in deep learning. In *Proceedings of the 30th International Conference on International Conference on Machine Learning - Volume 28*, ICML'13, pages III–1139–III–1147. JMLR.org, 2013.

[24] Tianbao Yang, Qihang Lin, and Zhe Li. Unified convergence analysis of stochastic momentum methods for convex and non-convex optimization. 04 2016.